Environ Sci Pollut Res (2014) 21:8336–8367
DOI 10.1007/s11356-014-2783-1

Electrochemical advanced oxidation processes: today and tomorrow. A review

Ignasi Sirés · Enric Brillas · Mehmet A. Oturan · Manuel A. Rodrigo · Marco Panizza

Received: 19 February 2014 / Accepted: 10 March 2014 / Published online: 2 April 2014

Abstract In recent years, new advanced oxidation processes based on the electrochemical technology, the so-called electrochemical advanced oxidation processes (EAOPs), have been developed for the prevention and remediation of environmental pollution, especially focusing on water streams. These methods are based on the electrochemical generation of a very powerful oxidizing agent, such as the hydroxyl radical ($^{\bullet}$OH) in solution, which is then able to destroy organics up to their mineralization. EAOPs include heterogeneous processes like anodic oxidation and photoelectrocatalysis methods, in which $^{\bullet}$OH are generated at the anode surface either electrochemically or photochemically, and homogeneous processes like electro-Fenton, photoelectro-Fenton, and sonoelectrolysis, in which $^{\bullet}$OH are produced in the bulk solution. This paper presents a general overview of the application of EAOPs on the removal of aqueous organic pollutants, first reviewing the most recent works and then looking to the future. A global perspective on the fundamentals and experimental setups is offered, and laboratory-scale and pilot-scale experiments are examined and discussed.

Keywords EAOPs · Anodic oxidation · Electro-Fenton · Photoelectrocatalysis · Photoelectro-Fenton · Sonoelectrochemistry · Water treatment

Abbreviations

ACP	3-Amino-6-chloropyridazine
ADE	Air diffusion electrode
AMI	3-Amino-5-methylisoxazole
AO	Anodic oxidation
AOP	Advanced oxidation process
BDD	Boron-doped diamond
BZQ	*p*-Benzoquinone
CF	Carbon felt
CNT	Carbon nanotube
COD	Chemical oxygen demand (mg of oxygen L^{-1})
DSA	Dimensionally stable anode
e^-	Electron
e^-_{CB}	Electron in the conduction band
E_{anod}	Anodic potential (V)
EAOP	Electrochemical advanced oxidation process
E_{cat}	Cathodic potential (V)
EF	Electro-Fenton
GC-MS	Gas chromatography coupled to mass spectrometry
h	Planck constant (6.626×10^{-34} m^2 kg/s)
HPLC	High-performance liquid chromatography
h^+_{VB}	Positively charged vacancy or hole in the valence band
MMO	Mixed metal oxides
PEC	Photoelectrocatalysis
PEF	Photoelectro-Fenton
R	Organic compound
ROS	Reactive oxygen species

Responsible editor: Philippe Garrigues

I. Sirés · E. Brillas
Laboratori d'Electroquímica dels Materials i del Medi Ambient, Departament de Química Física, Facultat de Química, Universitat de Barcelona, Martí i Franquès 1-11, 08028 Barcelona, Spain

M. A. Oturan
Laboratoire Géomatériaux et Environnement (LGE), Université Paris-Est, EA 4508, 5 bd Descartes, 77454 Marne-la-Vallée Cedex 2, France

M. A. Rodrigo
Department of Chemical Engineering, Faculty of Chemical Sciences and Technologies, Universidad de Castilla La Mancha, Edificio Enrique Costa, Campus Universitario s/n, 13071 Ciudad Real, Spain

M. Panizza (✉)
Department of Civil, Chemical and Environmental Engineering, University of Genoa, P.le J.F. Kennedy 1, 16129 Genoa, Italy
e-mail: marco.panizza@unige.it

RVC Reticulated vitreous carbon
SE Sonoelectrochemistry
SPEF Solar photoelectro-Fenton
TOC Total organic carbon (mg of carbon L^{-1})
US Ultrasounds
))) Ultrasounds

Greek symbols
λ Wavelength (nm)
ν Frequency (Hz)

Introduction

In recent decades, the rapid growth of public awareness about environmental problems has induced many governments to introduce legislation that prescribes and limits the emission of pollutants. This has been reflected in a notable increase in both research and the number of businesses concerned with the treatment of industrial effluents. Because of the extremely diverse features of industrial waste that usually contains a mixture of organic and inorganic compounds, no universal strategy of reclamation is feasible and it mainly depends on the nature and concentration of pollutants (Fig. 1). As to the treatment of effluents polluted with organic compounds, biological oxidation is certainly the cheapest process, but the presence of toxic or biorefractory molecules may hinder this approach. The traditional incineration method poses problems of emission if the treatment conditions are not perfectly controlled, and above all, it can be conveniently applied only for concentrated solutions (Fig. 1). Chemical oxidation using chlorine, ozone, or hydrogen peroxide is currently used for the treatment of biorefractory contaminants or at least to decompose them into harmless or biodegradable products. However, in some reactions, the intermediate products remain in the solution and they may entail a similar or even higher toxicity than the initial compounds. In these cases, the pollutants can be removed using a special class of oxidation technique known as advanced oxidation processes (AOPs).

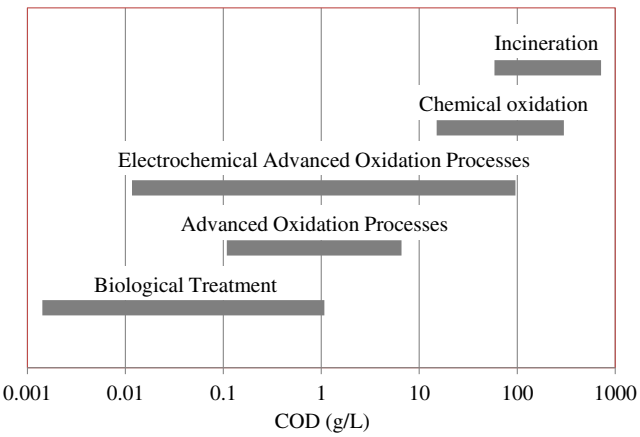

Fig. 1 Applicability of water treatment technologies based on the amount of organic load. Adapted from Fryda et al. (2003)

Table 1 Standard potential of some oxidizing species

Oxidizing agent	Standard potential (V vs. SHE)
Oxygen (molecular)	1.23
Chlorine dioxide	1.27
Chlorine	1.36
Ozone	2.08
Oxygen (atomic)	2.42
Hydroxyl-radical	2.80
Fluorine	3.06
Positively charged hole on TiO_2	3.2

Within the framework of liquid polluted streams, AOPs can be broadly defined as aqueous phase oxidation methods based on the intermediacy of highly reactive species (primarily but not exclusively) in the mechanisms leading to the destruction of the target pollutant. The hydroxyl radical ($^{\bullet}OH$) is a powerful oxidant (Table 1) which is able to nonselectively destroy most organic and organometallic contaminants until their complete mineralization into CO_2, water, and inorganic ions. These radicals react rapidly with organics (R) mainly by the abstraction of a hydrogen atom (aliphatics) or the addition on an unsaturated bond (aromatics) to initiate a radical oxidation chain:

$$RH + {}^{\bullet}OH \rightarrow H_2O + {}^{\bullet}R \quad (1)$$

$$ {}^{\bullet}R + O_2 \rightarrow ROO^{\bullet} \quad (2)$$

$$ROO^{\bullet} + RH \rightarrow ROOH + {}^{\bullet}R \quad (3)$$

$$ArH + {}^{\bullet}OH \rightarrow ArH(OH)^{\bullet} \quad (4)$$

$$ArH(OH)^{\bullet} + {}^{\bullet}O_2 \rightarrow [ArH(OH)OO]^{\bullet} \quad (5)$$

$$[ArH(OH)OO]^{\bullet} \rightarrow ArH(OH) + HO_2^{\bullet} \quad (6)$$

As summarized in Table 2, a large number of AOPs has been developed, including nonphotochemical and photochemical methods. The AOPs are successfully applied mainly for the treatment of wastewaters, but they are also used in many fields including groundwater treatment, soil remediation, municipal wastewater sludge conditioning, as well as odor and taste removal from drinking water.

In recent years, new AOPs based on the electrochemical technology, i.e., the so-called electrochemical advanced

Table 2 Main AOPs and related reactions involving the production of $^{\bullet}OH$

	Reactions
Dark AOPs	
Ozone at elevated pH	$3O_3+OH^-+H^+ \rightarrow 2^{\bullet}OH+4O_2$
Ozone+hydrogen peroxide	$2O_3+H_2O_2 \rightarrow 2^{\bullet}OH+3O_2$
Ozone+catalyst	$O_3+Fe^{2+}+H_2O \rightarrow Fe^{3+}+OH^-+^{\bullet}OH+O_2$
Fenton	$Fe^{2+}+H_2O_2 \rightarrow Fe^{3+}+OH^-+^{\bullet}OH$
Photo-assisted AOPs	
Ozone/UV	$O_3+H_2O+h\nu \rightarrow O_2+H_2O_2$
Hydrogen peroxide/UV	$H_2O_2+h\nu \rightarrow 2^{\bullet}OH$
Ozone/H_2O_2/UV	The addition of H_2O_2 to the O_3/UV process accelerates the decomposition of ozone, which results in an increased rate of $^{\bullet}OH$ generation
Photo-Fenton	$Fe^{2+}+H_2O_2+h\nu \rightarrow Fe^{3+}+OH^-+^{\bullet}OH$
	$Fe(OH)^{2+}+h\nu \rightarrow Fe^{2+}+^{\bullet}OH$
	$Fe(OOCR)^{2+}+h\nu \rightarrow Fe^{2+}+CO_2+R^{\bullet}$
Heterogeneous photocatalysis (TiO_2/UV)	$TiO_2+h\nu \rightarrow TiO_2(e^-+h^+)$
	$h^++H_2O \rightarrow {}^{\bullet}OH+H^+$
	$e^-+O_2 \rightarrow O_2^{-\bullet}$

oxidation processes (EAOPs), have been developed (Fryda et al. 2003; Martínez-Huitle and Ferro 2006; Brillas et al. 2009; Panizza and Cerisola 2009a; Sirés and Brillas 2012). The EAOPs provide several advantages for the prevention and remediation of pollution problems because the electron is a clean reagent. Other advantages include high energy efficiency, amenability to automation, easy handling because of the simple equipment required, safety because they operate under mild conditions (room temperature and pressure), and versatility because they can be applied to effluents with chemical oxygen demand (COD) in the range of 0.1 to 100 g L^{-1} (Fig. 1). The main drawbacks of some of these technologies include the costs related to the electrical supply, the low conductance of many wastewaters that require the addition of electrolytes, and the loss of activity and shortening of the electrode lifetime by fouling due to the deposition of organic material on their surface. More specific advantages and disadvantages of the technologies will be discussed later.

Key EAOPs include anodic oxidation (AO), in which heterogeneous $^{\bullet}OH$ are generated at the anode surface, as well as electro-Fenton (EF), photoelectro-Fenton (PEF), and sonoelectrochemistry (SE), in which homogeneous $^{\bullet}OH$ are produced in the bulk solution. It is also possible to couple various EAOPs such as the AO with EF, PEF, or SE to produce both heterogeneous and homogeneous $^{\bullet}OH$.

The growing interest of academic and industrial communities in EAOPs is reflected in the high number of publications in peer-reviewed journals, patents, and international conferences. Figure 2a illustrates that more than 50 % of the papers

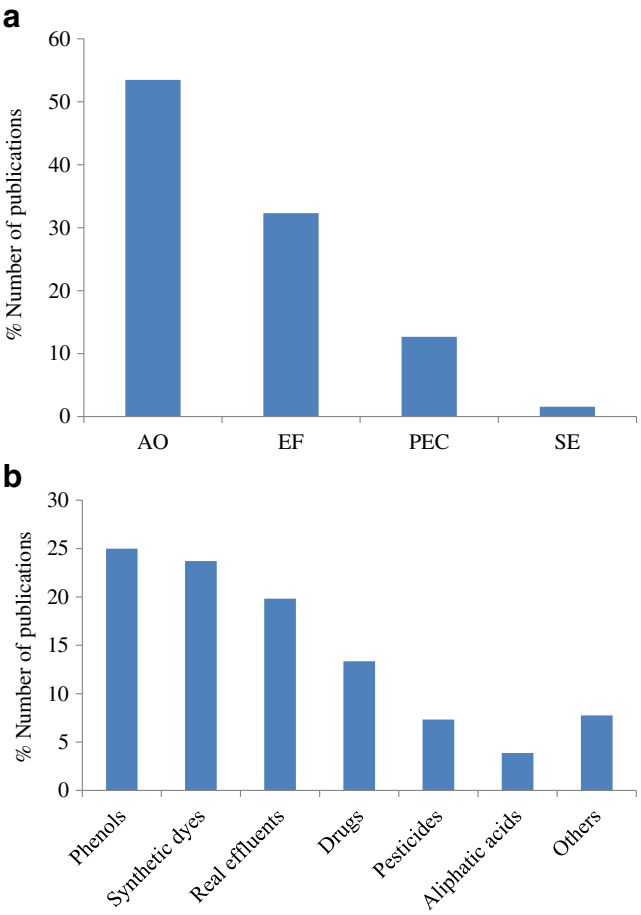

Fig. 2 Percentage of publications devoted to the EAOPs in the last 3 years. Distribution by **a** electrochemical techniques: anodic oxidation (*AO*), electro-Fenton (*EF*), photoelectrocatalysis (*PEC*), and sonoelectrochemistry (*SE*) and **b** type of residue

published in the last 3 years are devoted to the AO, in particular using the innovative boron-doped diamond (BDD) anode. Many papers studied the EF and PEF processes, while only few researches are focused in the less conventional but evolving SE processes.

The efficiency and flexibility of the EAOPs have been proven by the wide diversity of effluents treated, as shown in Fig. 2b, including either synthetic solutions containing phenols (Cañizares et al. 2003, 2004; Polcaro et al. 2003; Panizza and Cerisola 2009b), dyes (Panizza and Cerisola 2008; Martínez-Huitle and Brillas 2009; Rodriguez et al. 2009; Moreira et al. 2013), pesticides (Polcaro et al. 2005; Flox et al. 2007; Oturan et al. 2008; Panizza et al. 2008; Borràs et al. 2013), and drugs (Sirés et al. 2006a, 2007a; Isarain-Chávez et al. 2010) or real/industrial effluents (Panizza et al. 2006; Cañizares et al. 2006, 2007a; Malpass et al. 2008; Panizza and Cerisola 2010). Despite the large number of publications on the EAOPs and the very good results obtained in laboratory-scale tests, their practical application for the treatment of organic pollutants is still insufficient. But nowadays, given the intensive investigations that have improved

the electrocatalytic activity and stability of electrode materials, optimized reactor geometry, and deepened knowledge about reactor hydrodynamics, the EAOPs have reached an advanced stage of development and, recently, some pilot-scale or full-scale plants have been effectively commercialized for the disinfection and purification of wastewater polluted with organic compounds.

To date, one of the most developed large-scale applications of EAOPs is the automated disinfection of swimming pool water using BDD anodes. In this field, dedicated products such as Oxineo® and Sysneo® have been developed for private and public pools. Compared with the other disinfection methods, these systems have the advantages that there is no chlorine smell, no accumulation of chemicals in the pool, no need of anti-algae, and there is a residual action to avoid nonregular or jagged disinfections. Many of these systems have been already installed in private pools all over the world and several public pools and spas in Europe.

CONDIAS and Advanced Diamond Technologies Inc. develop and supply equipment for EAOPs, sold with the trademark of CONDIACELL® and Diamonox®, respectively, which are based on AO with BDD anode. Typical applications of these cells are (a) water disinfection and (b) industrial wastewater treatment. Some details of the Diamonox® system are reported in Fig. 3. For water disinfection, these cells produce a mixture of oxygen-based agents, such as $^{\bullet}OH$ and ozone, directly by water electrolysis, providing high disinfection rate with low energy consumption, without the addition of chemicals and they can either be used as a firewall or for volume disinfection.

The treatment of industrial wastewater is based on the production of $^{\bullet}OH$ and other oxidants, such as chlorine, (per)bromate, persulfate, ozone, hydrogen peroxide, percarbonate, and others, directly on-site using only water, salt, and energy. The advantage of industrial wastewater treatment using these EAOPs is the possibility to degrade COD/total organic carbon (TOC) from a value of several hundred grams O_2 per liter to a minimum of a few milligrams O_2 per liter or even micrograms O_2 per liter, with the reduction of all organic water components by approximately 99 %. Some other advantages related to these processes are the possibility of combining EAOPs with common methods for wastewater treatment to achieve an optimal cost-effective operation and their easy modular adaptation and scale-up.

Another full-scale application of EAOPs is the EctoSys®, which is an extremely efficient system that provides a reliable and sustainable disinfection of the ballast water in an economical and ecological manner. By applying electricity to the special electrodes, disinfectants are produced from the water directly in the piping to eliminate bacteria and organisms. In water with low salinity, the EctoSys® unit produces only $^{\bullet}OH$ as active substances, while in brackish water or seawater, it produces short-living $^{\bullet}OH$ and chlorine/bromine.

In 2007, a BDD electro-oxidation pilot plant (Fig. 4) was installed in Marelo (Cantabria, Spain) for the treatment of landfill leachates using traditional and advanced oxidation technologies (Anglada et al. 2009, 2010, 2011; Urtiaga et al. 2009). The plant was constituted by an aerobic treatment followed by chemical Fenton oxidation and a final AO treatment. The latter consists of an electrochemical reactor with BDD anodes of 1.05 m^2. The raw leachate contained approximately 2.8 g L^{-1} of TOC and 1.2 g L^{-1} of ammonia, and the overall efficiency in the combined system was 99 % of organic matter mineralization: 50 % of the initial TOC was degraded in the aerobic treatment, 35 % in the Fenton process, and the remaining 15 % in the final electro-oxidation step. The ammonia removal efficiency was greater than 90 %, with 50 % being due to the electrochemical treatment, since the Fenton process was unable to reduce the ammonia concentration.

This paper presents a general overview of the application of EAOPs on the removal of organic compounds, starting each section with a revision of the very last years and then giving a

Fig. 3 Some details of the Diamonox® system. Reprinted with permission from Advanced Diamond Technologies Inc.

Fig. 4 EAOP pilot plant for the treatment of landfill leachate in Marelo (Cantabria, Spain) (Anglada et al. 2009, 2010, 2011; Urtiaga et al. 2009)

look to the future. A global perspective on the fundamentals and experimental setups is offered, and laboratory and pilot plant experiments are examined and discussed.

Production of oxidants by electrolysis and their role in mediated anodic oxidation

One of the key points to explain the high efficiencies reached by EAOPs in the removal of organic pollutants is the understanding of the role depicted by mediated oxidation processes in the overall oxidation carried out during the treatment. Mediated oxidation in EAOPs can be understood as the oxidation of pollutants contained in wastewater by the chemical reaction between these compounds and the oxidants produced previously on the electrode surfaces. Thus, AO does not only lead to the direct oxidation of organic pollutants on the anode surface but it also promotes the formation of huge amounts of oxidants which can act not only on the surface of the electrodes but extend the oxidation process to the bulk solution of the treated waste (Panizza and Cerisola 2009a). The type and extension of the production of oxidants depend on many inputs, being the most relevant the electrode material and the occurrence of suitable raw matter for the production of oxidants in the wastewater. Their influence on the efficiency of EAOPs is very important because the oxidation of pollutants is extended from the vicinity of the electrode surface to the bulk of the electrolyte. However, it should be taken into account that these oxidants largely affect the mechanisms of the oxidation of pollutants and, occasionally, they can lead to the formation of unwanted intermediates or final stable products. Sometimes, the species that promote the formation of oxidants are not contained in the wastewater but added as reagents, which results in well-known and very effective processes. One of the most interesting examples is the treatment of wastes with Ag(II), whose formation was demonstrated to be very effective with conductive diamond electrodes (Panizza et al. 2000).

However, the most referenced example of mediated electrochemical oxidation arises from the effect of chlorides on the oxidation of organics. Chlorides are commonly contained in most wastewater flowstreams and they are known to be easily oxidized to chlorine by many types of anode materials (Eq. 7). This gaseous oxidant diffuses into the wastewater and forms hypochlorite and chloride in the reaction medium by disproportionation (Eqs. 8 and 9). Deprotonation of hypochlorous acid produces hypochlorite (Eq. 10). Since hypochlorite is the primary final product, in literature it is common to find the direct transformation of chloride into hypochlorite instead of the complete set of reactions (Eq. 11). However, the oxidation in that media is carried out by a mixture of reagents and the particular concentration of each species depends on the concentration and pH.

$$2\ Cl^- \rightarrow Cl_2 + 2\ e^- \tag{7}$$

$$Cl_2 + H_2O \rightarrow HClO + H^+ + Cl^- (\text{acidic medium}) \tag{8}$$

$$Cl_2 + 2\ OH^- \leftrightarrows ClO^- + Cl^- + H_2O (\text{alkaline medium}) \tag{9}$$

$$HClO + OH^- \leftrightarrows ClO^- + H_2O \tag{10}$$

$$Cl^- + H_2O \rightarrow ClO^- + 2\ H^+ + 2\ e^- \tag{11}$$

The resulting mixture (chlorine, hypochlorite, and hypochlorous acid) is highly reactive with many organics, being efficient for their mineralization (Comninellis and Nerini 1995; Panizza and Cerisola 2003). However, it is also known to form many organochlorinated species as intermediates and final products that can be even more harmful than the raw pollutant (Comninellis and Nerini 1995). Total depletion of these species is frequently very difficult and even the formation of low-molecular-weight products such as chloroform becomes a very significant problem because it could lead to additional treatments, increasing significantly the total cost of the remediation (Cañizares et al. 2003).

This is a negative and common example of the action of oxidants that does not exclude the promotion of the mediated oxidation processes in EAOPs, but alerts about some drawbacks and limitations of use. Thus, even with chlorides, when no organochlorinated by-products can be formed or when the oxidation of pollutants such as cyanide is aimed, the formation

of chlorinated oxidants is a significant advantage and allows increasing the effectiveness of EAOPs. This is clearly observed in Fig. 5 (obtained from the data of Cañizares et al. 2005a), where the electrochemical oxidation of cyanide synthetic wastes using sulfate-supporting and chlorine-supporting electrolytes and three different anode materials is compared in terms of COD removal. As it can be clearly observed, degradation of cyanide is much faster when chloride is contained in the synthetic waste. Likewise, it can be observed that anode material does not behave as a simple sink of electrons but it has a clear role in the reactivity of the system.

Nevertheless, and despite the fact that chlorine-mediated oxidation is very well known, it is not the only case of mediated oxidation processes and, of course, it is not the most significant one. Thus, when the objective is focused on the promotion of mediated oxidation, three important aspects should be taken into account:

- Direct electrochemical production of oxidants on the anode surface from non-oxidant species contained in the waste and the transport of these species toward the bulk (wastewater). The raw matter for the production of oxidants should be contained in the wastewater or dosed, and typically, it can be an ion (i.e., chloride, sulfate, etc.), an organic pollutant (acetic acid), dissolved gasses (oxygen), or even water.
- Effect of the raw oxidants produced electrodically on the organic pollutants.
- Activation of oxidants in the bulk, that is, the formation of highly reactive species from poorly reactive oxidants.

These three points will be studied in the following sections. Figure 6 shows a comprehensive summary of the main processes occurring during the oxidation of a pollutant contained in wastewater. It includes the mass transport of species from the bulk of the waste to the electrode surface and vice versa, and the main oxidation mechanisms which will be explained in this section, including direct oxidation and different types of mediated oxidation that typically occur during EAOPs.

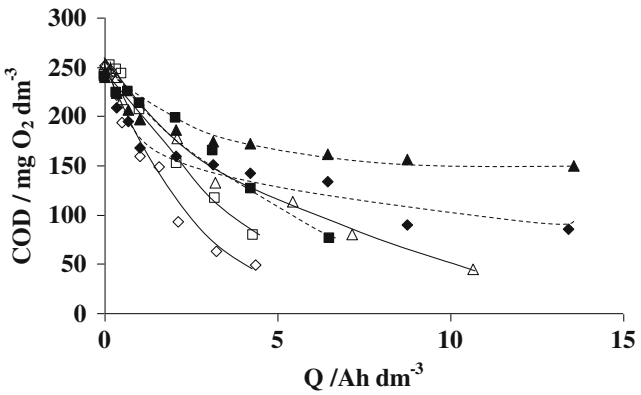

Fig. 5 Changes in the COD concentration during the electrochemical oxidation of synthetic wastes polluted with cyanide (375 mg NaCN L^{-1}). Supporting electrolyte: 0.05 M Na_2SO_4 (*black triangle* DSA, *black diamond* Pb/PbO_2, *black square* *p*-Si-BDD) and 0.05 M NaCl (*white triangle* DSA, *white diamond* Pb/PbO_2, *white square* *p*-Si-BDD). Adapted from Cañizares et al. (2005a)

Direct electrochemical production of oxidants

For the formation of oxidants in electrochemical wastewater treatment processes, three main points should be considered:

- Direct oxidation of species on the anode surface, involving the formation of radical species that combine to produce stable oxidants.
- Oxidation of water to $^{\bullet}OH$ and further attack of this powerful oxidant to species promoting the formation of radicals. Then, the combination of radicals leads to the production of stable oxidants.
- Reduction of oxygen to produce hydrogen peroxide on the cathode surface.

In the following subsections, a detailed description of these three mechanisms is going to be carried out.

Production of oxidants from direct oxidation processes

The first process pointed out in this subsection is the direct oxidation of species on the anode surface with the subsequent formation of radical species that combine to produce stable oxidants. This is known to occur for many species present in wastewater, in particular for chlorine and peroxo species, and also for ferrates. With some anode materials like diamond or PbO_2 coatings, the formation of radicals from anions such as sulfate (Eq. 12), phosphate (Eq. 13), carbonate (Eq. 14), and even acetic acid is promoted. By this mechanism, the formation of chloride radicals (Eq. 15) can also be explained (Bergmann 2010). These processes are also known to occur with other electrode materials such as platinum, but the efficiency observed is much worse and concentrations produced are quite insignificant to produce an effect on the results of the treatment process (Cañizares et al. 2009).

$$SO_4^{2-} \rightarrow (SO_4^{-})^{\bullet} + e^{-} \quad (12)$$

$$PO_4^{3-} \rightarrow \left(PO_4^{2-}\right)^{\bullet} + e^{-} \quad (13)$$

$$CO_3^{2-} \rightarrow (CO_3^{-})^{\bullet} + e^{-} \quad (14)$$

$$Cl^{-} \rightarrow Cl^{\bullet} + e^{-} \quad (15)$$

These radicals can combine based on the reactions shown in Eqs. 16, 17, 18, and 19, which explains the occurrence of

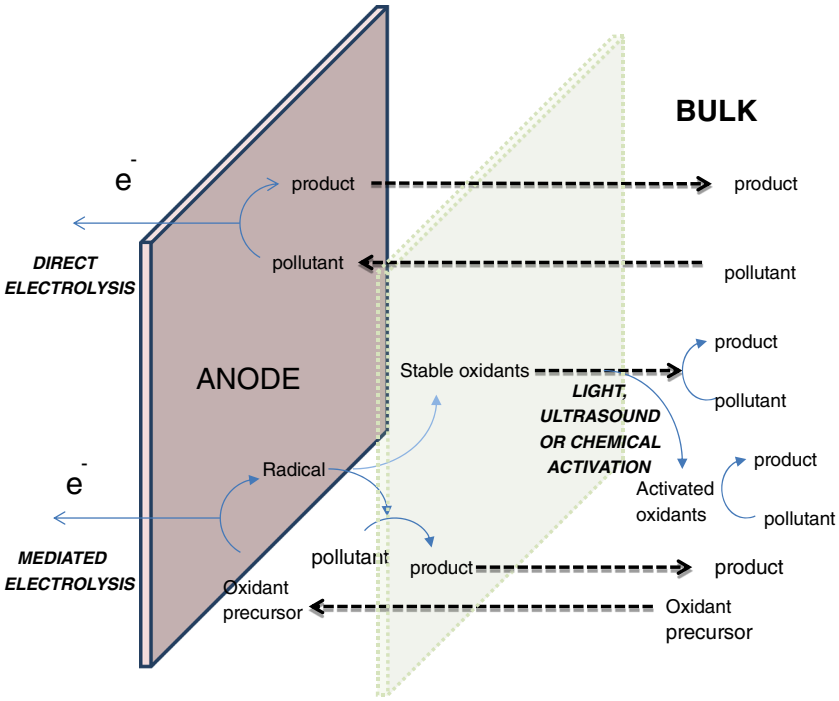

Fig. 6 A conceptual approach to mediated oxidation in EAOPs

the stable oxidants in the reaction media, including peroxosulfates (Serrano et al. 2002), peroxophosphates (Cañizares et al. 2005b), peroxocarbonates (Ruiz et al. 2009), and chlorine (Bergmann 2010).

$$(SO_4^{-})^{\bullet} + (SO_4^{-})^{\bullet} \rightarrow S_2O_8^{2-} \quad (16)$$

$$\left(PO_4^{2-}\right)^{\bullet} + \left(PO_4^{2-}\right)^{\bullet} \rightarrow P_2O_8^{4-} \quad (17)$$

$$(CO_3^{-})^{\bullet} + (CO_3^{-})^{\bullet} \rightarrow C_2O_6^{2-} \quad (18)$$

$$Cl^{\bullet} + Cl^{\bullet} \rightarrow Cl_2 \quad (19)$$

Regarding chlorine, it is important to keep in mind that the efficiency is particularly high in electrolysis with some mixed metal oxide (MMO) anodes in which this process is known to be promoted with respect to the water oxidation (dimensionally stable anode [DSA]-type electrodes). As mentioned previously, this process produces a very active oxidation mixture, although it is not always a good way to remove organic pollutants because it promotes the formation of organochlorinated intermediates and final products. In addition, this reaction mixture can promote the formation of chlorates. This process is not always electrochemically based, but it is also chemically activated by a well-known disproportionation reaction (Eq. 20) and it is stimulated with the aging of the reaction mixture (Bolyard et al. 1992). Chlorate is usually an unwanted product in the effluent from an EAOP, and its formation could also prevent the use of the EAOP technology in various applications.

$$3\ ClO^{-} \rightarrow ClO_3^{-} + 2\ Cl^{-} \quad (20)$$

Regarding direct oxidation, an unresolved case is the formation of ferrates, which have been used to explain the better efficiencies of some EAOPs when iron is present in the treated wastewater, even in electrocoagulation processes (Phutdhawong et al. 2000). However, conditions used in EAOPs are far from those required to produce them efficiently from Eq. 21, and it is very difficult to explain this observation in light of the present knowledge (Sáez et al. 2008).

$$Fe^{3+} + 4\ H_2O \rightarrow FeO_4^{2-} + 8\ H^{+} + 3\ e^{-} \quad (21)$$

Production of oxidants from hydroxyl radical mediated processes

For the second process under discussion in this subsection, the mediated production of oxidants by the action of $^{\bullet}OH$ formed electrodically, it is important to know more about the production of such radicals in the reaction media. $^{\bullet}OH$ is an intermediate in the AO of water to oxygen (Eq. 22) that is rarely detected in the reaction media because it combines chemically to components of the anode surface before forming oxygen. In addition, it may be rapidly transformed into hydrogen

peroxide (Eq. 23) and into hydroperoxyl radical (Eq. 24) (Oturan et al. 2012).

$$H_2O \rightarrow {}^{\bullet}OH + H^+ + e^- \quad (22)$$

$$2\,{}^{\bullet}OH \rightarrow H_2O_2 \quad (23)$$

$${}^{\bullet}OH + H_2O_2 \rightarrow HO_2{}^{\bullet} + H_2O \quad (24)$$

The oxidation of water to oxygen is typically considered an undesired side reaction in the electrochemical treatment of pollutants because it seriously affects the efficiency of the process, increasing significantly the operation costs (it leads to a nonvaluable product). Nevertheless, in various works (Kapałka et al. 2007, 2008), it has been stated that this oxygen may have a positive effect on the oxidation of organics because it may help induce the mineralization of organics, contributing to explain the high efficiencies of the electrolysis of organics. Anyway, there is a consensus in the role of ${}^{\bullet}OH$ as primary responsible for the high efficiencies of electrolyses with some types of electrodes. At this point, the electrodes in which ${}^{\bullet}OH$ are not effective because they are not free on their surface were defined as active electrodes in a pioneering work of the group of Comninellis (Gandini et al. 1999). However, for some electrodes classified as non-active, it has been proposed that ${}^{\bullet}OH$ cannot combine with the components of their surface and then, during a very short time, they are available to oxidize organics or other species such as anions contained in waste (Marselli et al. 2003). This explains the formation of radical species and the increased efficiency in the production of oxidants when these anode materials are used, which even push some research not only for the treatment of wastewater (Panizza et al. 2001; Weiss et al. 2008a) but also for the industrial production of these oxidants. Some of the reactions promoted by ${}^{\bullet}OH$ are summarized in Eqs. 25, 26, and 27 and some of the products formed after the combination of radicals can be explained by formerly stated Eqs. 16, 17, 18, and 19 (Cañizares et al. 2009).

$$O_2 + 2\,{}^{\bullet}OH \rightarrow O_3 + H_2O \quad (25)$$

$$HSO_4{}^- + {}^{\bullet}OH \rightarrow (SO_4{}^-)^{\bullet} + H_2O \quad (26)$$

$$HPO_4{}^{2-} + {}^{\bullet}OH \rightarrow \left(PO_4{}^{2-}\right)^{\bullet} + H_2O \quad (27)$$

In addition, some new oxidants can be formed by the combination of ${}^{\bullet}OH$ and the new radicals formed by their action (Weiss et al. 2008b). Eqs. 28, 29, and 30 show some examples.

$$(SO_4{}^-)^{\bullet} + {}^{\bullet}OH \rightarrow HSO_5{}^- \quad (28)$$

$$(H_2PO_4)^{\bullet} + {}^{\bullet}OH \rightarrow H_3PO_5 \quad (29)$$

$$CO_3{}^{-\bullet} + {}^{\bullet}OH \rightarrow HCO_4{}^- \quad (30)$$

This explains the formation of many new types of oxidants with this non-active materials, and this also justifies the higher concentration measured. It also allows explaining the formation of some undesirable species such as chlorates and perchlorates in the electrolysis of wastes containing chlorides with non-active electrodes, as shown in Eqs. 31, 32, 33, and 34 (Sánchez-Carretero et al. 2011), and it may also shed light on the formation of rare species such as perbromate, as shown in Eq. 35 (Sáez et al. 2010a).

$$Cl^- + {}^{\bullet}OH \rightarrow ClO^- + H^+ + e^- \quad (31)$$

$$ClO^- + {}^{\bullet}OH \rightarrow ClO_2{}^- + H^+ + e^- \quad (32)$$

$$ClO_2{}^- + {}^{\bullet}OH \rightarrow ClO_3{}^- + H^+ + e^- \quad (33)$$

$$ClO_3{}^- + {}^{\bullet}OH \rightarrow ClO_4{}^- + H^+ + e^- \quad (34)$$

$$BrO_3{}^- + {}^{\bullet}OH \rightarrow BrO_4{}^- + H^+ + e^- \quad (35)$$

Production of hydrogen peroxide on the cathode

The third way to produce oxidants in the reaction media is very interesting because it complements very efficiently the two approaches described previously. It consists in the production of hydrogen peroxide by reduction of oxygen on the cathode surface (Zhou et al. 2012). From the thermodynamic point of view, hydrogen peroxide is less powerful than oxygen but, kinetically, at room temperature, it is much more efficient. This means that a way to enhance the efficiency of an EAOP is promoting the formation of hydrogen peroxide by the otherwise unproductive reaction at the cathode. Production of hydrogen peroxide by the reduction of oxygen develops in most cathode materials, but to increase efficiency, some three boundary points are required, that is, points in which cathode, water, and oxygen are in contact. For this reason, a special type of porous cathode, known as gas diffusion cathode, is employed for this application. Additional information about this process is going to be given in other sections of this manuscript where Fenton processes are described.

Effect of the raw oxidants produced electrochemically on reaction performance

There are many works in the literature in which the effects of the reaction media or small changes in the reaction media on the treatment results are assessed. These works demonstrate that reaction media have a large influence on results and that unexpected results were sometimes obtained (Panizza and Cerisola 2005; Sirés et al. 2006b; Martínez-Huitle and Brillas 2009; Sirés and Brillas 2012). Some illustrative examples are highlighted, as follows:

(i) There are no significant differences in the oxidation of organics in sulfate-supporting and phosphate-supporting electrolytes using BDD anodes, as can be clearly observed in Fig. 7, in which the influence of COD and supporting electrolyte composition on the instantaneous current efficiency is shown (Cañizares et al. 2005c). For many years, phosphate media were used as an inert media because peroxophosphate production was not expected. The absence of significant differences between electrolyses carried out with organic solutions containing sulfates and phosphates allow realizing that peroxophosphates were produced efficiently, leading to the proposal of a method for their manufacture (Cañizares et al. 2007b).

(ii) The effect of current density is much smaller than expected based on predictions of electrochemical mass transport models (Polcaro et al. 2002, 2009). This is also observed in Fig. 7 in which no significant differences are observed between results obtained for the removal of 4-chlorophenol (4-CP) by AO with BDD anode at current densities within the range of 150–600 A m^{-2}.

(iii) The comparative AO of the same organic pollutant in chloride-supporting media with DSA and BDD anodes reveals a better performance of DSA electrodes in spite of the expected best characteristics of BDD. With BDD anode, chlorides are not only oxidized to chlorine but also to chlorate and perchlorate. At room temperature, these latter oxidants are not very effective and this explains the best performance of DSA, in which only chlorine and hypochlorite formation is promoted.

(iv) With non-active electrodes, such as conductive diamond coatings, it is very difficult to find an inert supporting electrolyte and merely perchlorate seems to be the only supporting electrolyte in which no reactivity is obtained.

One important point regarding the oxidants produced during the electrochemical treatment of a particular wastewater is that they are not always detected in the reaction media although their effect is clearly observed by comparison of efficiencies when the composition of the raw wastewater is modified. In this context, the detection and quantification of oxidants during an electrolytic treatment can be understood as an indication of the low reactivity of the oxidant with the pollutants contained in the wastewater and not as an improvement of the process performance. The best way to obtain a highly efficient process is to promote the activation of the oxidants produced electrochemically, either by chemical, sonochemical, or photochemical methods.

Activation of oxidants produced electrochemically

As it has been described in the previous section, the reactivity of many of the raw oxidants produced in EAOPs with organics is not very high and some sort of activation is often required to obtain a clear improvement of the process. As an example of the improvement that such an activation can yield, an illustrative example can be considered: the transformation

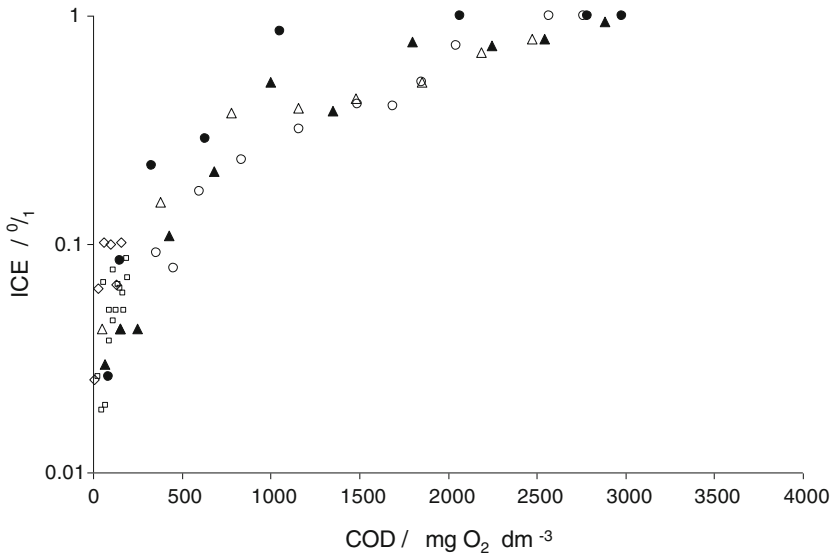

Fig. 7 Changes in the instantaneous current efficiency (*ICE*) with COD in the electrochemical oxidation of wastes containing 4-CP (C^0 = 15 mM). *Black circle* pH 2, 5,000 mg $Na_2SO_4L^{-1}$, 25 °C, 30 mA cm^{-2}; *white circle* pH 2, 5,000 mg $Na_2SO_4L^{-1}$, 25 °C, 15 mA cm^{-2}; *black triangle* pH 2, 5,000 mg $Na_2SO_4L^{-1}$, 25 °C, 60 mA cm^{-2}; *white diamond* pH 12, 5,000 mg $Na_2SO_4L^{-1}$, 25 °C, 30 mA cm^{-2}; *white triangle* pH 2, 5,000 mg $Na_2SO_4L^{-1}$, 60 °C, 30 mA cm^{-2}; *white square* pH 2, 3,333 mg $Na_3PO_4L^{-1}$, 25 °C, 30 mA cm^{-2}. Adapted from Cañizares et al. (2005c)

of peroxosulfate into sulfate radicals that may increase the process performance very significantly because the sulfate radical typically reacts 10^3–10^5 times faster than the persulfate ions (Tsitonaki et al. 2010). At this point, activation means the formation of highly reactive species from the oxidants contained in the wastewater and, as it has been pointed out in Fig. 6, there are three different modes:

- Chemical activation;
- Activation by light irradiation;
- Activation by ultrasound (US) irradiation.

Chemical activation of oxidants

Chemical activation is one of the most important ways to enhance the effectiveness of an oxidant. It involves the combination of the oxidant produced electrochemically with another species (not necessary an oxidant), which leads to the production of a third, very reactive species. This is the case of the well-known Fenton processes (Brillas et al. 2009) which will be described afterward in this manuscript. In these processes, a metal ion (most likely iron(II), but also other transition metal cations) catalyzes the formation of $^{\bullet}OH$ in the bulk from the decomposition of hydrogen peroxide. As it is known, hydrogen peroxide is a weak oxidant, while $^{\bullet}OH$ is one of the most active oxidants known.

Another example of chemical activation is the synergistic combination of oxidants that results when ozone and hydrogen peroxide are combined (Table 2). This mixture also results in the production of important concentrations of $^{\bullet}OH$ that explains the better efficiency of the processes in which the formation of both oxidants is promoted.

The activation of hydrogen peroxide is very important in EAOPs because this species is produced on the cathode of the electrochemical cell, and then, it can double the efficiency of the oxidation processes if properly activated (raw hydrogen peroxide is not very active).

Activation by light irradiation

Light irradiation activation means the promotion in the formation of highly active species by UV light irradiation. This irradiation can be applied naturally (solar driven) or artificially (using UV lamps). Excluding heterogeneous photoelectrocatalytic processes on the surface of the anodes (typically based on the use of MMO anodes with titanium dioxide as one of the components) because they will be reviewed afterward, in this subsection, light irradiation stands only for the decomposition of oxidants in the bulk upon the action of light. Thus, the photoactivation (or light-assisted decomposition) of electrochemically generated reactive species, such as H_2O_2 or O_3, by the reactions proposed in Eqs. 36 and 37 (Pelegrini et al. 2000) is well known.

$$H_2O_2 + h\nu \rightarrow 2^{\bullet}OH \tag{36}$$

$$H_2O + O_3 + h\nu \rightarrow 2^{\bullet}OH + O_2 \tag{37}$$

However, there are more processes with relevance in EAOPs (Bergmann et al. 2002). Radical species are expected to be produced by light decomposition of peroxo compounds such as peroxophosphates, peroxosulfates, and peroxocarbonates. As an example, the production of sulfate radical from persulfate is shown in Eq. 38 (Lin et al. 2011; Shih et al. 2012).

$$S_2O_8^{2-} + h\nu \rightarrow 2(SO_4^{-})^{\bullet} \tag{38}$$

The production of radicals from chlorine has also been assessed in the literature (Oliver and Carey 1977; Chan et al. 2012), and it has been demonstrated that, under non-extreme pH, hydroxyl and chlorine radicals are the main products resulting from the light-assisted degradation of hypochlorite (Eqs. 39 and 40).

$$ClO^{-} + \quad + h\nu \rightarrow O^{-\bullet} + Cl^{\bullet} \tag{39}$$

$$O^{-\bullet} + H_2O \rightarrow OH^{-} + 2^{\bullet}OH \tag{40}$$

Activation by ultrasound irradiation

US irradiation as a treatment technology consists in the production of a cyclic sound pressure with a frequency greater than the upper limit of human hearing (20,000 Hz) in wastewater. Unlike what one could expect, the main effect of US irradiation on chemicals is not based on the direct interaction of the mechanical acoustic field with chemical bonds of molecules, but it is supported by the formation, growth, and implosive collapse of bubbles irradiated with US (ultrasonic cavitation). This phenomenon takes place in a very short moment and space and it can be considered as adiabatic (Hiller et al. 1992). As a consequence, high temperatures and pressures are reached inside the bubble due to gas compression. This increase in temperature and pressure generates a huge concentration of energy in a very small place known as a hot spot (Flannigan and Suslick 2005). This energy is dispersed to the surroundings so that the gas temperature in the hot spot quickly returns to the ambient value. However, during a very short time, it can produce significant changes in chemical composition of the hot spot and can form new radical species and components, and so, it can increase the reactivity of the system (Rooze et al. 2013). Hence, the formation of $^{\bullet}OH$ is known and, based on what has been described previously, this will account for the formation of many other oxidizing species.

In addition, a further advantage in the electrochemical system comes from the increase in the mass transport produced by the mechanical acoustic field which improves the efficiency of processes in which the diffusion of pollutants limits the rate of direct AO. The most representative and studied process that demonstrates such assertion is sonoelectro-Fenton (SEF), which will be discussed in the "Sonoelectro-Fenton" section.

Prospects

Perspectives of enhancing mediated oxidation for future EAOP developments seem favorable. As it has been pointed out along this section, mediated oxidation processes become the key point to attain an enhancement in the efficiency of EAOPs. Actually, it is not the production of oxidants, but their activation in the reaction media, which is the most interesting topic of research. Costs of US technology are very high and improvements in efficiency are not always as good as to propose their coupling with EAOPs. This is a direct consequence of the huge amounts of energy dispersed as heat or mechanical energy with this technology. Any novelty in this topic has to come from a more efficient use of energy to promote the formation of many hot spots in which radical reactions could be started up. In contrast, light irradiation already seems to be a very promising alternative with good perspectives to be used in the near future. The synergistic effect of the activation of oxidants has been clearly demonstrated and the energy irradiated is much lower than that applied in US irradiation.

Chemical and electrochemical generation of hydroxyl radicals based on Fenton's chemistry

The Fenton's reagent, a mixture of H_2O_2 and Fe(II), constitutes the basis of the chemical generation of the strong oxidant $^{\bullet}OH$. A pioneering work was reported by Fenton in 1894 on the oxidation of tartaric acid (Fenton 1894). Fenton observed the enhancement of the oxidation power of H_2O_2 in the presence of iron(II) ions. Later, in the 1930s, Haber and Weis undertook a detailed work to clarify the mechanism of the reaction between H_2O_2 and Fe^{2+} (Eq. 41) and showed that Fenton's reagent led to the formation of $^{\bullet}OH$ (Haber and Weiss 1934). They concluded that the catalytic decomposition of H_2O_2 by ferrous ion through a radical and chain mechanism constitutes the origin of the oxidizing power of the Fenton's system. Eq. 41 was then named "Fenton's reaction."

$$Fe^{2+} + H_2O_2 \rightarrow Fe^{3+} + {}^{\bullet}OH + OH^- \quad (41)$$

More recent studies have demonstrated that Fenton's reaction could be applied to the degradation/destruction of different types of organic pollutants (Sun and Pignatello 1993a; Gallard et al. 1998; Pignatello et al. 2006), and because of its significant development during the twentieth century in the treatment of wastewater, several review papers have focused on this process (Walling 1998; Bautista et al. 2008).

Fenton's reaction as a source of hydroxyl radicals

Sun and Pignatello (1993b) showed that Fenton's reaction can be applied in acidic pH of 2.8–3.0 to efficiently produce $^{\bullet}OH$. At this pH, Fenton's reaction (Eq. 41) can be propagated by the catalytic behavior of the Fe^{3+}/Fe^{2+} couple. Indeed, under excess of H_2O_2, ferrous ions can be generated based on the following reactions (Eqs. 42 and 43) to catalyze Fenton's reaction (Haber and Weiss 1934):

$$Fe^{3+} + H_2O_2 \rightarrow Fe^{2+} + HO_2^{\bullet} + H^+ \quad (42)$$

$$HO_2^{\bullet} + Fe^{3+} \rightarrow Fe^{2+} + O_2 + H^+ \quad (43)$$

However, the $HO_2^{\bullet}$ radical has a lower oxidation power compared with $^{\bullet}OH$, and consequently, it is less reactive toward organic pollutants. In addition, these reactions are much slower than Fenton's reaction and lead to the accumulation of Fe^{3+} in the medium, causing the formation of sludge in the form of $Fe(OH)_3$. In addition to pH value, the concentrations of H_2O_2 and Fe^{2+} and their ratio ($[H_2O_2]/[Fe^{2+}]$) have a significant role regarding the practical efficiency of the Fenton process and have to be optimized for each specific case (Bouafia-Chergui et al. 2010), since for high concentrations, the reagents H_2O_2 and Fe^{2+} react with $^{\bullet}OH$ through the following wasting reactions, Eqs. 44 and 45, that significantly impair process efficiency:

$$H_2O_2 + {}^{\bullet}OH \rightarrow H_2O + HO_2^{\bullet} \quad (44)$$

$$Fe^{2+} + {}^{\bullet}OH \rightarrow Fe^{3+} + OH^- \quad (45)$$

The Fenton process was applied to the oxidation of organics and treatment of wastewaters starting from the 1960s (Brown et al. 1964), and many applications were developed in the 1990s (Gogate and Pandit 2004; Pignatello et al. 2006). However, several studies have shown the limitations of this process in several cases, and the following drawbacks have been highlighted: (i) high cost and risks due to the provision, storage, and transport of H_2O_2, (ii) accumulation of iron sludge that must be removed at the end of the treatment, and (iii) lower mineralization efficiency due to the presence of wasting reactions and, as a consequence, the potential formation of intermediates that are more toxic than raw pollutants. Therefore, to improve the practical application for the

treatment of wastewaters, the Fenton process has been coupled to other physicochemical processes like coagulation–flocculation, membrane filtration, and biological oxidation to eliminate organic pollutants more effectively (Lucas et al. 2007).

Electro-Fenton process: principles and running

The EF process is among the most known and popular EAOPs and constitutes an indirect electrochemical manner to generate $^{\bullet}OH$ in aqueous solutions. It was developed and extensively applied over the last decade, particularly by Brillas' and Oturan's groups since the 2000s (Brillas et al. 2000, 2009; Oturan 2000). This process has been developed to achieve the implementation of a new and powerful advanced oxidation method by avoiding the drawbacks of the chemical Fenton process. Indeed, it can be defined as an electrochemically assisted Fenton process. $^{\bullet}OH$ is produced via the Fenton's reaction (Eq. 41), in which Fenton's reagent is electrochemically generated in situ, avoiding the use of high quantities of H_2O_2 and iron(II) salt.

The H_2O_2 production rate is one of the crucial parameters of process efficiency, since the rate of Fenton's reaction is predominantly controlled by this parameter. It can be continuously supplied to the wastewater solution to be treated in an electrochemical reactor from the two-electron cathodic reduction of oxygen gas, directly injected as compressed air, as expressed in Eq. 46:

$$O_{2(g)} + 2\ H^+ + 2\ e^- \rightarrow H_2O_2 \quad (46)$$

The current efficiency of H_2O_2 production is generally not very high and depends on some factors such as operating conditions (O_2 solubility, temperature, and pH) and cathode properties. It can be destroyed by parasitic chemical decomposition (Eq. 47), cathodic reduction (divided cell) (Eq. 48), or AO (undivided cell) (Eqs. 49 and 50), resulting in a slower accumulation in the bulk. Therefore, the use of optimal operating conditions (acidic pH, ambient temperature, etc.) and an appropriate cathode material are important to obtain better production rates.

$$2\ H_2O_2 \rightarrow O_{2(g)} + 2\ H_2O \quad (47)$$

$$H_2O_2 + 2\ H^+ + 2\ e^- \rightarrow 2\ H_2O \quad (48)$$

$$H_2O_2 \rightarrow HO_2^{\bullet} + H^+ + e^- \quad (49)$$

$$HO_2^{\bullet} \rightarrow O_{2(g)} + H^+ + e^- \quad (50)$$

Several cathode materials such as mercury, graphite, carbon–polytetrafluoroethylene (PTFE) O_2 diffusion, and three-dimensional electrodes like carbon felt (CF), activated carbon fiber, reticulated vitreous carbon (RVC), carbon sponge, and carbon nanotubes (CNT) (Oturan et al. 1992; Brillas et al. 1995; Alverez-Gallegos and Pletcher 1999; Oturan 1999) were tested for H_2O_2 production. Based on the results published nowadays, 3D CF and carbon–PTFE O_2-fed cathodes seem to constitute better cathode material for efficient H_2O_2 generation; the use of Hg has been disregarded owing to its potential toxicity.

The second component of Fenton's reagent, i.e., the Fe^{2+} ion, is initially introduced in a catalytic amount (typically 0.1 mM) in the form of ferrous (or ferric) salts and is regenerated electrocatalytically (Eq. 51) from the reduction of Fe^{3+} formed by Fenton's reaction.

$$Fe^{3+} + e^- \rightarrow Fe^{2+} \quad (51)$$

Thus, Fenton's reagent is continuously produced in the solution to be treated in a catalytic manner, producing $^{\bullet}OH$ via Fenton's reaction to ensure the destruction of organic pollutants in aqueous medium. Formed $^{\bullet}OH$ quickly reacts in the bulk with organics, leading to their oxidation/mineralization following Eqs. 52 and 53.

$$\text{Organic pollutants} + {}^{\bullet}OH \rightarrow \text{oxidation intermediates} \quad (52)$$

$$\text{Intermediates} + {}^{\bullet}OH \rightarrow \rightarrow \rightarrow CO_2 + H_2O + \text{inorganic ions} \quad (53)$$

Compared with the classical Fenton process, the main advantages of the EF process are (i) in situ and controlled generation of Fenton's reagent (cost-effectiveness), thus avoiding the risks related to transport, storage, and handling of H_2O_2, (ii) elimination of parasitic reactions that waste $^{\bullet}OH$ (very low Fenton's reagent concentration), (iii) total mastership of the processing by current or potential control, (iv) possibility of controlling the degradation kinetics and performing mechanistic studies, and (v) almost total mineralization of organics including the intermediates.

Influence of applied current on the oxidation/mineralization efficiency

A number of operating parameters, such as solution pH, applied current, catalyst (Fe^{2+}) concentration, supporting electrolyte, organic load, etc., influence process efficiency. Although the optimal value of pH is well known to be 2.8 (Sun and Pignatello 1993b), the process can effectively occur within the range $2.5<pH<3.5$.

The nature and concentration of the used catalyst have a significant role in the EF process. To be used in EF, the catalyst should be one of the forms of the redox couple, both forms being soluble in water to allow the electrogeneration of the

reduced form in homogeneous medium. To clarify the effect of the nature of the catalyst, a number of $M^{z+}/M^{(z-1)+}$ couples were investigated (Brillas et al. 2004; Pimentel et al. 2008; Balci et al. 2009; Oturan et al. 2010; Salazar et al. 2012). Cu^{2+} showed good catalytic characteristics in combination with Fe^{2+} or Fe^{3+} (Brillas et al. 2004; Salazar et al. 2012), but when used alone, high concentrations are needed for obtaining the same efficiency than Fe^{2+} (Oturan et al. 2010). Mn^{2+} was found to be a good candidate in place of iron ions when their use is compromised (Balci et al. 2009). Co^{3+} and Ag^{+} exhibited catalytic behavior similar to that of Fe^{2+} (Pimentel et al. 2008), but their use should be disregarded due to their ecotoxicity. Usually, Fe^{2+} (or Fe^{3+}) behaves as the best catalyst in the EF process particularly because it acts efficiently at lower concentrations, typically around 0.1 mM. In this case, the oxidation/mineralization of organic pollutants occurs efficiently at low concentrations, but the effectiveness of the process decreases with increasing Fe^{2+} concentration, in particular at long treatment times (Abdessalem et al. 2008), due to the enhancement of the rate of the parasitic reaction (Eq. 45).

The applied current (or current density) is the most important operating parameter of the EF process, since it governs the rate of generation of H_2O_2 (Eq. 46), as well as the regeneration rate of Fe^{2+} (Eq. 51) and, consequently, the rate of generation of $^{\bullet}OH$ from Fenton's reaction (Eq. 41). In general, the rate of the process increases with applied current since more $^{\bullet}OH$ are formed at a given time. By contrast, the applied current cannot be increased indefinitely, since high current values promote parasitic reactions, leading to the decrease in current and process efficiencies. In particular, the applied current should not reach the reduction potential of H_2O_2 (Eqs. 49 and 50) to preserve it in the solution. Another wasting reaction that becomes enhanced when increasing the applied current is the evolution of H_2 at the cathode. Figure 8 clearly shows the effect of the applied current in the case of the oxidation of 0.125 mM of the herbicide picloram in aqueous medium at pH 3.0 by the EF process (Özcan et al. 2008). We observed that the oxidation kinetics was enhanced with applied current from 50 to 300 mA, although the increase in decay kinetics was not proportional to current due to the gradual enhancement of the parasitic reactions. A further increase in applied current did not yield a positive effect on the oxidation kinetics, as shown for the case of 500 mA. We noted that the oxidation process was very fast, and the total disappearance of picloram was reached within less than 5 min for applied current values of 200, 300, and 500 mA. Therefore, the value of 200 mA can be considered as the optimal value to minimize the energy consumption at practically the same reaction time.

The classical EF process has been initiated by using Pt as the anode. In this case, the process occurs mainly in the bulk solution by $^{\bullet}OH$ generated homogeneously through Fenton's reaction. Recently, a significant enhancement has been

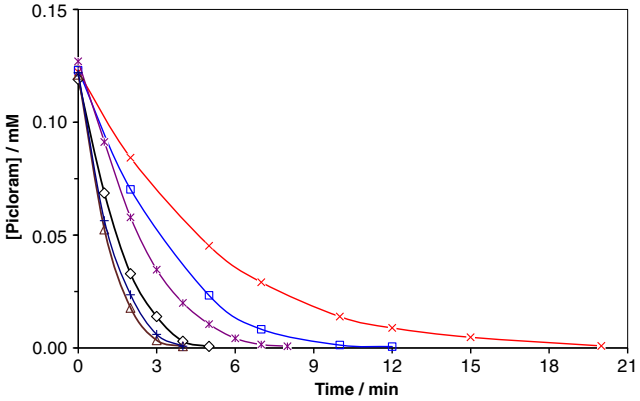

Fig. 8 Effect of applied current on the degradation kinetics of 0.125 mM picloram in aqueous medium at pH 3 and room temperature by the EF process: *multiplication sign* 30 mA, *white square* 60 mA, *asterisk* 100 mA, *white diamond* 200 mA, *white triangle* 300 mA, *plus sign* 500 mA. $[Fe^{3+}] = 0.1$ mM, $[Na_2SO_4] = 50$ mM. Reprinted with permission from Özcan et al. (2008). Copyright 2008 Elsevier

attained by replacing the Pt anode with the more effective BDD anode. The use of the BDD anode enables the EF process to become more potent, since this anode allows generating supplementary heterogeneous $^{\bullet}OH$ (BDD($^{\bullet}OH$)) at its surface (Eq. 54), in addition to those produced in bulk solution from Fenton's reaction. The use of the BDD anode in the EF process also has three other advantages, as follows: (i) the oxidizing power of BDD($^{\bullet}OH$) is higher than other anodes due to a larger O_2 overvoltage, (ii) BDD($^{\bullet}OH$) is physisorbed at the surface and thereby more easily available (compared with the Pt anode), and (iii) the high oxidation window of the BDD anode (approximately 2.5 V) allows the direct oxidation of organic pollutants (Brillas and Martínez-Huitle 2011).

$$BDD + H_2O \rightarrow BDD(^{\bullet}OH) + H^+ + e^- \quad (54)$$

A recent and interesting study clearly showing the improvement of the EF process by using the BDD anode reports the mineralization of the refractory herbicide atrazine (Oturan et al. 2012). Indeed, a large variety of AOPs have been already applied to the oxidative degradation and/or mineralization of atrazine. However, in all cases, they yielded the persistent end product cyanuric acid as predominant by-product, with 40–60 % mineralization yields, corresponding to the mineralization of the side chains of the molecule. In contrast, when a BDD anode was used in the EF process, an almost total mineralization (97 % TOC removal) of atrazine aqueous solutions was obtained (Fig. 9). The significant mineralization power of EF with BDD anode relative to the classical process with Pt anode can be clearly appreciated. In addition, the authors showed in the same study that cyanuric acid, which was already reported as recalcitrant to $^{\bullet}OH$, can also be almost completely mineralized because of the action of BDD($^{\bullet}OH$) that is more potent than $^{\bullet}OH$ in the mineralization of some recalcitrant organics like carboxylic acids.

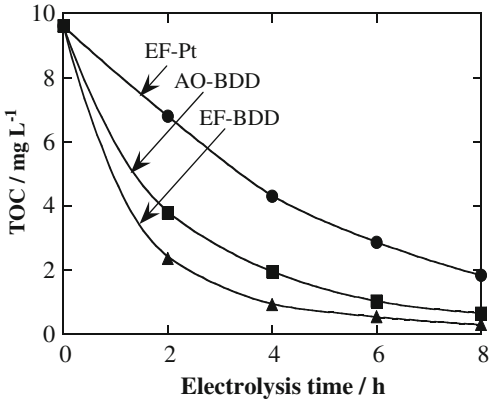

Fig. 9 TOC removal during the mineralization of 0.1 mM atrazine aqueous solution by the EF process using Pt and BDD anodes and CF cathode. *EF-Pt* electro-Fenton process with Pt anode, *AO-BDD* anodic oxidation using BDD anode, *EF-BDD* electro-Fenton process with BDD anode. Reprinted with permission from Oturan et al. (2012). Copyright 2012 Springer

Some recent applications

Since the publication of the first reports on the treatment of wastewaters by the EF process (Brillas et al. 2000; Oturan 2000), it has been significantly developed and applied to the treatment of a large variety of wastewaters polluted by toxic and/or persistent organic pollutants such as pesticides (Oturan et al. 2011; Zhao et al. 2012), synthetic dyes (Lahkimi et al. 2007; Khataee et al. 2009; Martínez-Huitle and Brillas 2009; Panizza and Oturan 2011), industrial pollutants (Panizza and Cerisola 2001; Bellakhal et al. 2006), pharmaceuticals and personal care products (Sirés et al. 2007b, 2010), landfill leachates (Zhang et al. 2006), reverse osmosis concentrates (Zhou et al. 2012), and many others. Among all these applications, three applications are especially detailed in the following paragraphs.

The first application deals with the effect of the chlorine atom substituent on the oxidation efficiency of the process (Oturan et al. 2009). This study reports the comparative kinetics of the degradation of several chlorophenols such as monochlorophenols (2-chlorophenol (2-CP) and 4-CP), dichlorophenols (2,4-dichlorophenol (2,4-DCP) and 2,6-dichlorophenol (2,6-DCP)), trichlorophenols (2,3,5-trichlorophenol (2,3,5-TCP) and 2,4,5-trichlorophenol (2,4,5-TCP)), 2,3,5,6-tetrachlorophenol (2,3,5,6-TeCP), and pentachlorophenol (PCP), using a CF cathode and a Pt anode. It was demonstrated that the number and the position of the chlorine atoms in the aromatic ring influence significantly the oxidation and mineralization kinetics of chlorophenols. This effect was evaluated in terms of apparent and absolute rate constants of the reaction between $^{\bullet}OH$ and chlorophenols. Apparent rate constants were obtained following the pseudo-first-order kinetics and have been found to decrease with the increase in the number of chlorine atoms, in the following sequence: 4-CP>2-CP>2,4-DCP>2,6-DCP>2,3,5-TCP>2,4,5-TCP>2,3,5,6-TeCP>PCP. Then, the absolute rate constants of the second-order reaction between chlorophenols and $^{\bullet}OH$ were determined by the competition kinetics method. The values of the absolute rate constants (k_{abs}) were in the $3.56–7.75\times10^{9}$ M^{-1} s^{-1} range, following the same sequence of the apparent rate constants (Table 3). The mineralization of several chlorophenols and of their mixture was also carried out by monitoring with TOC removal percentage. Results showed that more highly chlorinated phenols were more difficult to mineralize, with the mineralization rate decreasing when the number of chlorine atoms increased.

The second application focuses on the assessment of solution toxicity when treated by the EF process. Indeed, important efforts have been devoted to studies on the removal of a new class of emerging pollutants, the pharmaceuticals and personal care products, because of their occurrence in natural waters and their potentially toxic effects on aquatic species (Sirés et al. 2007b). The removal of many of these substances was studied, including treatment efficiency, determination of apparent and absolute rate constants, mechanistic assessments, and mineralization pathways (Oturan et al. 2009; Sirés et al. 2010; Dirany et al. 2011). A recent study devoted to the removal of the antibiotic sulfamethoxazole from water by the EF process focused on a special issue like the changes in the solution toxicity during treatment (Dirany et al. 2011). The evolution of the global toxicity of the treated solution was monitored by using the Microtox® bioluminescence method, in which toxicity is expressed as the inhibition percentage of the luminescence of *Vibrio fischeri* bacteria. Figure 10 highlights an interesting behavior during the EF treatment of sulfamethoxazole. Inhibition percentages were measured after the exposure of bacteria to the solution for 15 min. Inhibition curves obtained during the application of different applied currents exhibited different peaks appearing as a function of the treatment time. These inhibition peaks can be related to the formation of primary and then secondary or tertiary aromatic (and/or cyclic) intermediates formed during the treatment. The significant increase in global toxicity at the beginning of the treatment revealed the formation of some oxidation intermediates that were more toxic than the parent compound. This is a behavior often observed during the application of AOPs. Figure 10a shows a significant increase in the luminescence inhibition between approximately 10 min (for I=300 mA) and

Table 3 Absolute rate constants (k_{abs}) for the oxidation of chlorophenols by $^{\bullet}OH$ generated during the EF process (reprinted with permission from Oturan et al. 2009)

Chlorophenol	k_{abs} (10^{9}) M^{-1} s^{-1}
4-CP	7.75±0.07
2,6-DCP	6.13±0.05
2,4,5-TCP	5.72±0.05
2,3,5,6-TeCP	4.95±0.07
PCP	3.56±0.06

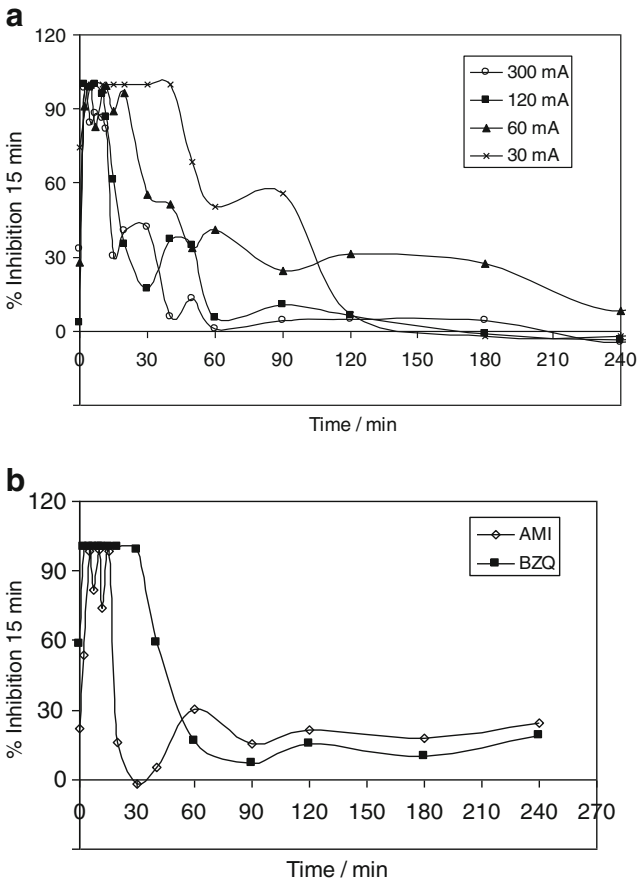

Fig. 10 Evolution of the inhibition of the *V. fischeri* bacteria luminescence during EF treatment, with Pt anode and CF cathode, of **a** sulfamethoxazole (*SMX*) aqueous solutions and **b** its cyclic derivatives 3-amino-5-methylisoxazole (*AMI*) and *p*-benzoquinone (*BZQ*) diluted aqueous solutions, after an exposure time of 15 min. V=250 mL, $[SMX]_0$=0.208 mM, $[AMI]_0$=0.016 mM, $[BZQ]_0$=0.018 mM, $[Fe^{2+}]$=0.2 mM, $[Na_2SO_4]$=50 mM, pH=3, I=30, 60, 120, and 300 mA in **a**, and I=60 mA in **b**. Reprinted with permission from Dirany et al. (2011). Copyright 2011 Springer

60 min (for I=30 mA) of treatment. Then, a rapid decrease occurs with the appearance/disappearance of minor inhibition peaks at electrolysis times of 30–180 min. As indicated by different curves, the solution toxicity was more quickly eliminated with higher current values. The time-related shifts of luminescence inhibition peaks with the current value can be explained by different formation rates of $^{\bullet}OH$, depending on the applied current. As explained previously in the "Influence of applied current on the oxidation/mineralization efficiency" section, the formation rate of $^{\bullet}OH$ is governed mainly by applied current and increases from 50 to 300 mA (Fig. 8). As a consequence, sulfamethoxazole and its by-products were mineralized more quickly, leading to a rapid decrease in solution toxicity. The high-performance liquid chromatography (HPLC) analyses indicated that 3-amino-5-methylisoxazole (AMI) and *p*-benzoquinone (BZQ) were the primary oxidation by-products of sulfamethoxazole. To clarify the relative toxicity of these intermediates, their diluted solutions were treated under the same operating conditions. Figure 10b was obtained from diluted solutions of AMI and BZQ effectively attained during the EF oxidation of sulfamethoxazole and demonstrated that both aromatic (and/or cyclic) intermediates were, at least partly, responsible for the increase in toxicity of sulfamethoxazole solutions because, at least, one of the major intermediates, like BZQ, is significantly more toxic than sulfamethoxazole toward *V. fischeri* bacteria.

The third application concerns the removal of the antibiotic drug sulfachloropyridazine from water and its mineralization pathway during the treatment of its aqueous solution by the EF process (Dirany et al. 2012). The suggested mineralization pathway includes 15 cyclic intermediates (identified by HPLC and gas chromatography coupled to mass spectrometry [GC-MS] analyses), 5 aliphatic carboxylic acids (oxalic, maleic, pyruvic, glyoxylic, and malic acids), and a mixture of released inorganic ions (Cl^-, SO_4^{2-}, NH_4^+, and NO_3^-). Based on the action of $^{\bullet}OH$ onto four different sites of sulfachloropyridazine, a detailed scheme for the complete mineralization of sulfachloropyridazine was proposed. The reaction of $^{\bullet}OH$ with this pharmaceutical yielded different primary cyclic by-products, shown as pathways A–D in Fig. 11. Pathways A and B involve the formation of five benzenesulfonamides promoted by consecutive hydroxylation steps with or without Cl^- release. Pathways C and D occur simultaneously and include the oxidative cleavage of the structure, leading to the formation of a dozen pyridazine and benzenic derivatives. Among these intermediates, 3-amino-6-chloropyridazine (ACP) and BZQ were detected as major intermediates. Successive hydroxylation of the primary intermediates weakens the structure and promotes ring breaking to yield carboxylic acids, accompanied by the release of inorganic ions like chloride, sulfate, ammonium, and nitrate. In addition, the time course of some available reaction intermediates such as ACP and BZQ was satisfactorily correlated with the toxicity profiles determined using the Microtox® method in terms of the inhibition of *V. fischeri* luminescence. ACP and BZQ, which are the predominant intermediates, were found responsible for the significant increase in toxicity during the first stages of treatment.

Prospects

The EF process emerged as an environmentally friendly AOP approximately 10 years ago, mainly in its two basic versions based on the nature of the cathode material: CF and carbon–PTFE gas diffusion electrode. Nowadays, there are several dozen groups studying and publishing works related to this process. It is very largely investigated at the laboratory scale, mainly in its two initial versions. The use of the emergent BDD anode significantly enhanced the oxidation power and mineralization efficiency due to the production of

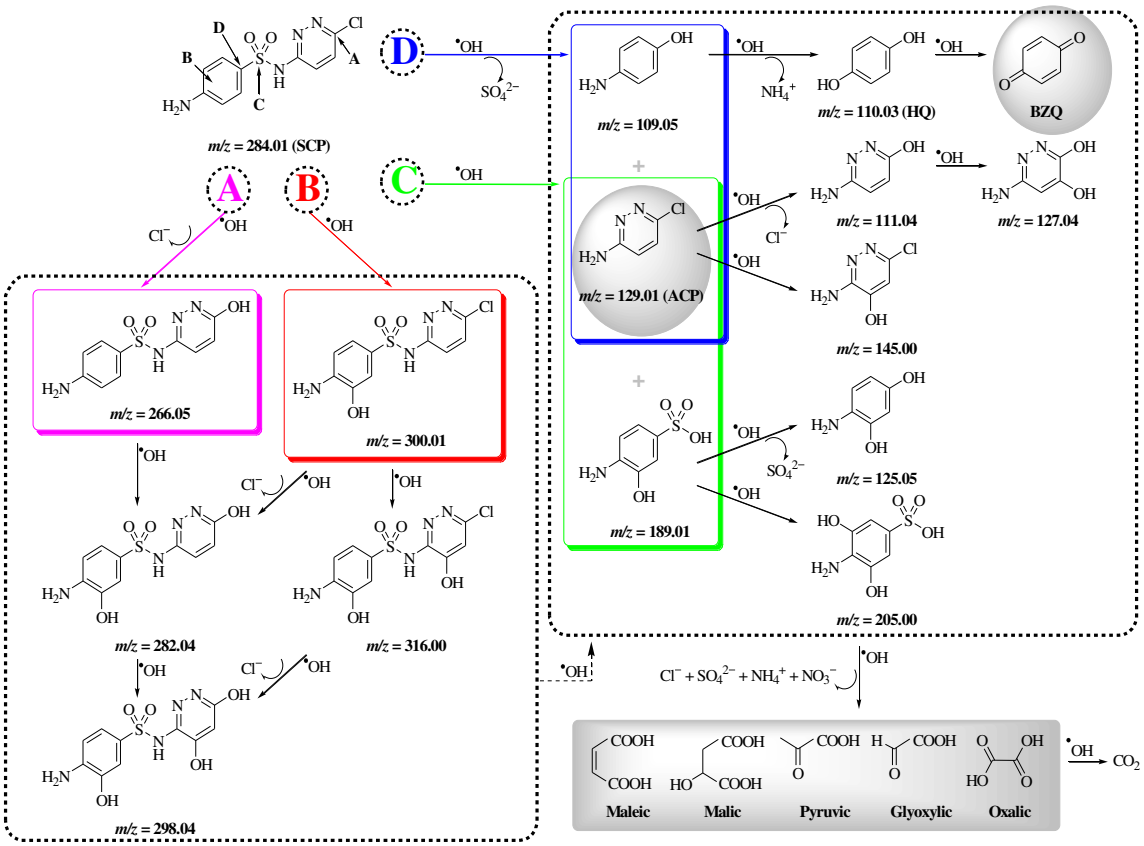

Fig. 11 Reaction pathways for the total mineralization of the drug sulfachloropyridazine by •OH generated during the EF process. Reprinted with permission from Dirany et al. (2012). Copyright 2012 American Chemical Society

supplementary •OH at the anode surface. Therefore, this technology becomes now mature enough for passing to pilot-scale reactor design and application to treatment of large volumes of wastewaters.

The first step will be the conception and design of a pilot-scale reactor. This conception can include combined processes to increase the effectiveness of the treatment. Both batch reactor and continuous (flow) reactor should be considered. The modeling of the process can be useful to optimize the operating parameters and predict the behavior of pollutants and can help in the economical and practical application to real wastewater treatment.

The design of a tubular reactor can constitute an interesting way to reach continuous treatment. A joint project focused on the coupling of EF with nanofiltration, in which a carbonaceous material is suggested as both filter and cathode, was recently applied for funding to the French ANR (National Research Agency) by three French universities (including the LGE Laboratory of Université Paris-Est) and a company of the field. The second step will consist of checking if the parameters optimized at the laboratory scale could be considered for the work in the pilot-scale reactor, before the industrial-scale reactor stage. Otherwise, the key parameters should be optimized at the pilot scale.

Coupling with a biological process as a pretreatment or posttreatment unit is another promising way for cost-effective treatment. Some recent studies have shown the feasibility of such coupling. Indeed, the EF process is able to transform toxic and/or biorefractory molecules to biodegradable species during a short treatment time. The complete mineralization of solutions thus obtained can then be achieved by biological treatment.

To develop cost-effective treatments, the use of green and cheap energy source based on sunlight-driven electrical power systems such as an EF reactor directly powered by photovoltaic panels can also be considered.

Photoelectrochemical processes

There is an increasing interest in the use of photoelectrochemical processes for water and wastewater remediation. These photo-assisted treatments are based on the irradiation of a contaminated solution or a photoactive electrode with UV or solar light (Brillas et al. 2009; Sirés and Brillas 2012; Daghrir et al. 2012a; Georgieva et al. 2012). UVA (λ=315–400 nm), UVB (λ=285–315 nm), and UVC (λ <285 nm) lights supplied by UV lamps as energy sources are

commonly employed. The intensity and wavelength of such radiations have a significant effect on the destruction rate of organic pollutants. However, the excessive economical cost of artificial light sources for the application of UV-assisted processes is worthy of consideration. This is solved in solar-assisted processes where sunlight (λ>300 nm) is used as a free, inexpensive and renewable energy source, although frequently the influence of this radiation has been assessed using a solar simulator device. Hereafter, the characteristics and main applications of the most interesting photoelectrochemical processes including PEF, solar photoelectro-Fenton (SPEF), and photoelectrocatalysis (PEC), as well as hybrid systems, are described.

Photoelectro-Fenton and solar photoelectro-Fenton

PEF with artificial UVA light and SPEF, its derived sunlight-assisted method, have been envisaged and widely developed by Brillas' group. These processes involve the treatment of the contaminated solution under EF conditions along with the simultaneous irradiation with UVA or solar light to accelerate the mineralization rate of organics. Oxidizing $^{\bullet}$OH are produced from Fenton's reaction (Eq. 41), while the undesired accumulation of refractory Fe(III) ions that decelerate the treatment is avoided by the reductive photolysis of $[Fe(OH)]^{2+}$, the predominant Fe(III) species in solution at pH 2.8–3.5, based on photo-Fenton reaction (Eq. 55), thereby regenerating Fe^{2+} (i.e., the catalyst in Fenton's reaction) and producing more radicals (Brillas et al. 2009; Sirés and Brillas 2012):

$$[Fe(OH)]^{2+} + h\nu \rightarrow Fe^{2+} + {}^{\bullet}OH \quad (55)$$

Radiation can also promote the photolysis of some oxidation intermediates or their Fe(III) complexes, allowing the regeneration of Fe^{2+} in photodecarboxylation reactions:

$$Fe(OOCR)^{2+} + h\nu \rightarrow Fe^{2+} + CO_2 + R^{\bullet} \quad (56)$$

$$2\ Fe(C_2O_4)_n^{(3-2n)} + h\nu \rightarrow 2\ Fe^{2+} + (2n-1)C_2O_4^{2-} + 2\ CO_2 \quad (57)$$

Brillas' group studied the degradation of drug residues like paracetamol (Sirés et al. 2006a), clofibric acid (Sirés et al. 2007c), ibuprofen (Skoumal et al. 2009), atenolol (Isarain-Chávez et al. 2010), and flumequine (Garcia-Segura et al. 2012), as well as the herbicide cyanazine (Borràs et al. 2013), using a small stirred and thermostated tank reactor containing solutions of 100 mL. A Pt or BDD anode and a carbon–PTFE gas diffusion cathode, all with 3 cm^2 area, were used. The cathode was fed with O_2 or air for continuous H_2O_2 production. In EF, PEF, and SPEF, 0.5 mM Fe^{2+} was usually added as catalyst. A 6-W UVA lamp of λ_{max}=360 nm was used in PEF, whereas the SPEF process was made under direct solar irradiation with an average UV intensity of approximately 31 W m^{-2}.

As an example, Fig. 12a shows the TOC decay vs. electrolysis time for the comparative EF, PEF, and SPEF treatments of 100 mL of 41 mg L^{-1} ibuprofen in 0.05 M Na_2SO_4 with 0.5 mM Fe^{2+} at pH 3.0, 33.3 mA cm^{-2}, and 25.0 °C (Skoumal et al. 2009). The performance of each process increased using a BDD anode instead of a Pt anode, as expected with the higher oxidizing power of BDD($^{\bullet}$OH) compared with Pt($^{\bullet}$OH) generated at the corresponding anode surface from water oxidation (Panizza and Cerisola 2009a). The UVA light in PEF enhanced EF degradation, reaching

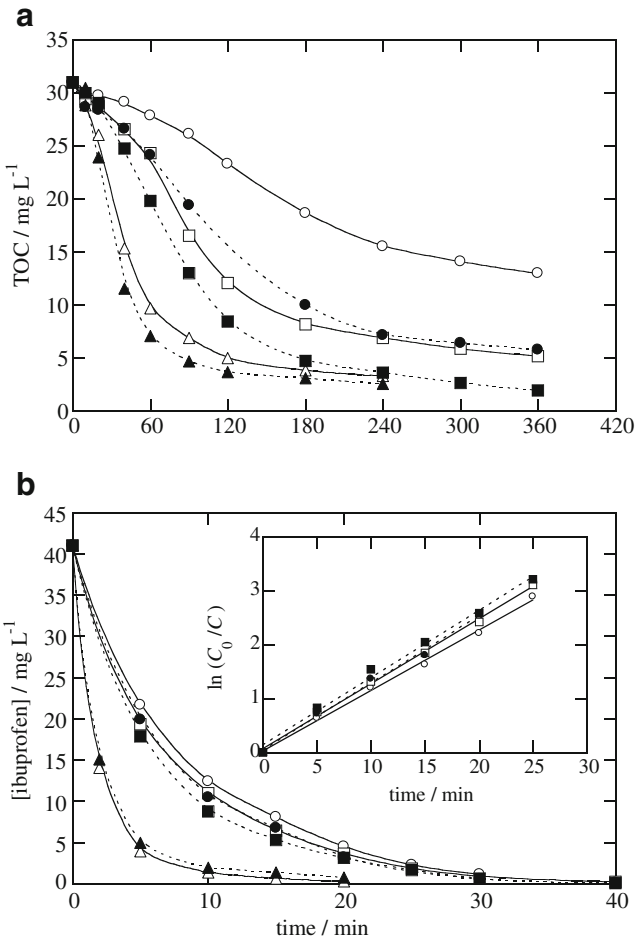

Fig. 12 **a** TOC decay and **b** concentration decay vs. time for the degradation of 100 mL of 41 mg L^{-1} ibuprofen (near saturation) in 0.05 M Na_2SO_4 with 0.5 mM Fe^{2+} at pH 3.0 using an O_2 diffusion cathode at 33.3 mA cm^{-2} and 25.0 °C. The *inset panel* of plot **b** presents the corresponding kinetic analysis considering that the drug follows a pseudo-first-order reaction. *White circle* EF with a Pt anode, *black circle* EF with a BDD anode, *white square* PEF with Pt and a 6-W UVA lamp, *black square* PEF with BDD under 6 W UVA radiation, *white triangle* SPEF with Pt, *black triangle* SPEF with BDD. Adapted from Skoumal et al. (2009)

even more quickly the almost total mineralization in SPEF. For all treatments, the optimal pH value was 3.0, close to the optimum pH of 2.8 for Fenton's reaction (Brillas et al. 2009), and no more than 0.5–1.0 mM Fe^{2+} had to be added. The mineralization current efficiency of SPEF trials was greater than that of EF and PEF assays, and it increased when current density decreased. Figure 12b shows that ibuprofen concentration was depleted at a similar rate in EF and PEF, in agreement with a pseudo-first-order reaction, yielding an apparent rate constant (k_1) of approximately 2.1×10^{-3} s^{-1}. The ibuprofen decay was significantly accelerated in SPEF, as expected if more $^{\bullet}OH$ is produced from the photolytic reaction (Eq. 55) due to the higher UV intensity of sunlight. GC-MS and reversed-phase HPLC analysis of treated solutions revealed the formation of aromatic products like 4-ethylbenzaldehyde, 4-isobutyl-acetophenone, 4-isobutylphenol, and 1-(1-hydroxyethyl)-4-isobutylbenzene. Ion exclusion HPLC allowed the identification and quantification of oxalic acid as the ultimate short-chain carboxylic acid accumulated to a larger extent. Indeed, it could not be removed by EF, but it disappeared quickly by PEF and much faster by SPEF due to the fast photolysis of its Fe(III) complexes, as shown in Eq. 57. This behavior explains the higher mineralization degree attained in PEF and SPEF (see Fig. 12a).

The use of Cu^{2+} as cocatalyst in EF and PEF was explored for the degradation of 157 mg L^{-1} paracetamol at pH 3.0 using a Pt/O_2 diffusion cell (Sirés et al. 2006a). The combination of 1 mM Fe^{2+}, 1 mM Cu^{2+}, and UVA light was unique, since it led to almost TOC removal after 4 h of electrolysis at 100 mA cm^{-2}. The synergistic effect of all catalysts promoting the quickest decontamination was explained considering that $^{\bullet}OH$ in the bulk destroys the Cu(II)–oxalate and Cu(II)–oxamate complexes, whereas the competitively formed Fe(III)–oxalate and Fe(III)–oxamate complexes are photolyzed by UVA light.

The studies performed with other pollutants (Sirés et al. 2007c; Isarain-Chávez et al. 2010; Garcia-Segura et al. 2012; Borràs et al. 2013) confirmed the superiority of PEF over analogous EF treatment and BDD over Pt. For example, for the mineralization of 100 mL of 179 mg L^{-1} clofibric acid with 1.0 mM Fe^{2+} of pH 3.0 using a Pt/O_2 diffusion cell at 100 mA cm^{-2}, 92 % TOC removal for PEF vs. only 73 % for EF was obtained. The use of BDD in PEF led to a quicker degradation, with more than 96 % TOC decay for the same current density at 4 h. A similar k_1 value of $(1.35\pm0.10)\times10^{-2}$ s^{-1} was obtained for all the EF and PEF treatments, a value much greater than that obtained for the AO process, thus confirming the higher reactivity of $^{\bullet}OH$ formed in the bulk to remove aromatics compared with that of Pt($^{\bullet}OH$) or BDD($^{\bullet}OH$). In addition, single Pt/air diffusion electrode (ADE) and BDD/ADE cells and their combinations with a Pt/CF cell were checked for the treatment of 100 mL of 158 mg L^{-1} atenolol with 0.5 mM Fe^{2+} at pH 3.0 (Isarain-Chávez et al. 2010). While in EF the combined cells led to a greater mineralization than the single cells because of the enhanced generation of the main oxidant $^{\bullet}OH$, in PEF, atenolol was mineralized at a similar rate using both kinds of cells because of the quick photolysis of the iron complexes under UVA irradiation. The GC-MS and HPLC analyses of solutions with aromatic pollutants treated by PEF corroborated that hydroxylation followed by the generation of short-chain carboxylic acids was the main degradation route. The photolysis of final Fe(III)–carboxylate complexes then explains the quickest mineralization by PEF.

Other authors have also shown the higher oxidation ability of PEF using electrolytic cells with different carbonaceous cathodes to generate H_2O_2 (Irmak et al. 2006; Peralta-Hernández et al. 2008; Wang et al. 2008, 2011; Dhaouadi and Adhoum 2009; Kaplan et al. 2011; Khataee et al. 2011). Thus, Irmak et al. (2006) treated 300 mL of an O_2-saturated 0.6 mM 4-chloro-2-methylphenol solution of pH 2.7 in the cathodic compartment of a divided cell equipped with a Pt gauze anode, a 3 cm×5 cm CF cathode, and a Nafion 117 membrane as separator. At a constant cathodic potential (E_{cat}) of −0.55 V/saturated calomel electrode (SCE) and 1.8 mM Fe^{2+}, they found a fast and complete degradation of the aromatic ring in the PEF system under UVC irradiation, with 41.7 % TOC decay and complete dechlorination after consumption of 141.4 C for 300 min. In EF, 280.7 C was consumed during 450 min of electrolysis to attain a similar removal of initial pollutant, but only yielding 14.9 % TOC removal and 89.3 % dechlorination. Similar results were obtained in the comparative EF and PEF degradations of 100 mL of 20 mg L^{-1} of the herbicide paraquat in an O_2-saturated solution with 0.05 M Na_2SO_4 and 0.2 mM Fe^{2+} at pH 3.0 and 100 mA using a Pt/CF cell illuminated with a 6-W UVA lamp (Dhaouadi and Adhoum 2009). HPLC analysis of electrolyzed paraquat solutions allowed the identification of three main aromatic intermediates that led to short-chain carboxylic acids, whereas the initial nitrogen was transformed into NO_3^- ion.

By contrast, Wang et al. utilized a cell equipped with a Ti/RuO_2 anode and an activated carbon fiber cathode to treat 450 mL of 200 mg L^{-1} of the azo dye Acid Red 14 (Wang et al. 2008) and 125 mL of 200 mg L^{-1} of the antibiotic sulfamethoxazole (Wang et al. 2011), using an O_2-saturated solution with 0.05 M Na_2SO_4 and 1 mM Fe^{2+} at pH 3.0 and 360 mA in both cases. After 6 h in EF conditions, TOC was reduced by 59 and 63 %, respectively, whereas the comparative PEF treatment with an 11-W UVA lamp led to 95 and 80 % mineralization. HPLC and GC-MS analyses allowed the detection of six aromatic products during sulfamethoxazole degradation by the PEF process, mainly formed from the hydroxylation of the aromatic and/or isoxazole ring, accompanied by the substitution of the amine group (on the aromatic

cycle) or methyl group (on the isoxazole ring) by $^{\bullet}OH$. Oxalic, maleic, oxamic, formic, and acetic acids were detected, and the initial organic nitrogen was converted into NH_4^+.

In view of the superiority of SPEF over PEF found in the stirred tank reactor, Brillas' group extended the study to pre-pilot plants aiming at further application at the industrial scale. The SPEF treatment of organics was first scaled up to a recirculation flow plant of 2.5 L with a BDD/O_2 diffusion cell coupled to a flat solar photoreactor (Flox et al. 2007; Guinea et al. 2010; Ruiz et al. 2011a, b; Salazar et al. 2011). Figure 13a, b shows a scheme of the flow plant and the cell used for these trials (Flox et al. 2007). The electrodes had an area of 20 cm^2, with a gap of approximately 1.2 cm.

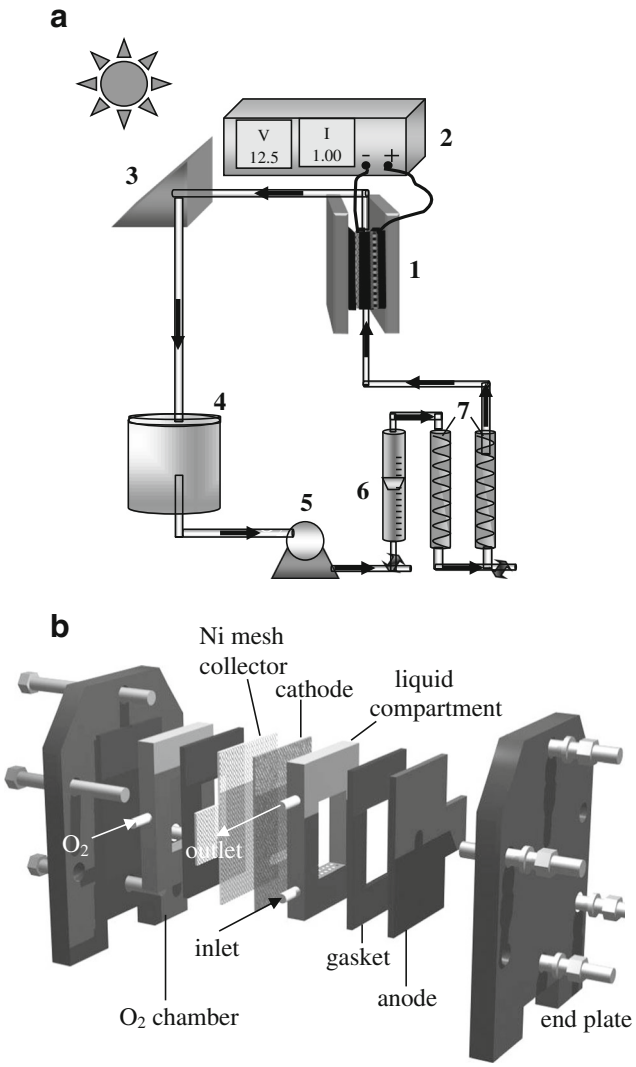

Fig. 13 Sketches of **a** the 2.5-L pre-pilot plant and **b** the single one-compartment filter–press electrochemical cell with a BDD anode and an O_2 diffusion cathode, both of 20 cm^2 exposed area, used for the SPEF degradation of organic pollutants in acid medium. In **a**, *1* flow cell, *2* power supply, *3* solar photoreactor, *4* reservoir, *5* peristaltic pump, *6* flow meter, *7* heat exchangers. Adapted from Flox et al. (2007)

The solar photoreactor was a polycarbonate box of 600 mL of irradiated volume, built up with a mirror at the bottom and tilted 30° from the horizontal. Solutions with 50–350 mg L^{-1} of TOC in 0.05–0.10 M Na_2SO_4 with 0.5 mM Fe^{2+} at pH 3.0, 50 mA cm^{-2}, and flow rate of 180–200 L h^{-1} were usually tested. As found in the stirred tank reactor, SPEF was much more potent to mineralize organics than AO and EF. For example, TOC was reduced by 95 % after 540 min of SPEF treatment of 100–637 mg L^{-1} of the herbicide mecoprop at 50 mA cm^{-2} (Flox et al. 2007). Similarly, almost total mineralization was achieved for the dyes Acid Yellow 36 (Ruiz et al. 2011a), Acid Red 88 (Ruiz et al. 2011b), Acid Yellow 9 (Ruiz et al. 2011b), Disperse Red 1 (Salazar et al. 2011), and Disperse Red 3 (Salazar et al. 2011) by SPEF. For all compounds, the SPEF efficiency increased at lower current density and higher pollutant content. The same trend was obtained for the energy consumption per unit TOC mass. This parameter was as high as 259 kWh(kg TOC)$^{-1}$ after 240 min of EF treatment of 100 mg L^{-1} TOC of Disperse Red 1 at 50 mA cm^{-2}, whereas it was reduced to 151 kWh(kg TOC)$^{-1}$ for the comparative SPEF treatment with >90 % mineralization (Salazar et al. 2011). This confirms that SPEF is much more economical than EF.

As found with the stirred tank, the performance of SPEF was enhanced from the combined use of Fe^{2+} and Cu^{2+} for the treatment of Disperse Blue 3 dye in 0.10 M Na_2SO_4 with a BDD/ADE cell in the flow plant (Salazar et al. 2012). Optimum conditions were found for 0.5 mM Fe^{2+}+0.1 mM Cu^{2+}. Figure 14a, b reveals that the presence of the cocatalyst led to >95 % TOC abatement in the presence and absence of 200 mg L^{-1} dye with energy consumption <80 kWh(kg TOC)$^{-1}$, more rapidly and less expensive than using 0.5 mM Fe^{2+} alone. This corroborates the aforementioned attack of $^{\bullet}OH$ on Cu(II)–carboxylate complexes, competitively formed with Fe(III)–carboxylate complexes.

In trials performed using the 2.5-L pre-pilot plant, it was found that the decay of all initial aromatics in EF and SPEF always followed a pseudo-first-order kinetics and the apparent rate constant k_1 increased at higher current density and lower pollutant content. The reaction pathways tend to be rather complex, like in the case of Disperse Blue 3, where up to 15 anthraquinonic and phthalic acid derivatives were identified (Salazar et al. 2012). Analysis of final carboxylic acids confirmed the quick removal of oxalic acid by photolysis of its Fe(III) complexes, but other recalcitrant acids like acetic and oxamic may slow down the mineralization processes (Flox et al. 2007; Guinea et al. 2010; Ruiz et al. 2011a, b; Salazar et al. 2011, 2012). The heteroatoms contained in the pollutants are usually released in the form of Cl^-, NH_4^+, and NO_3^- ions (Guinea et al. 2010; Ruiz et al. 2011a, b; Salazar et al. 2011, 2012).

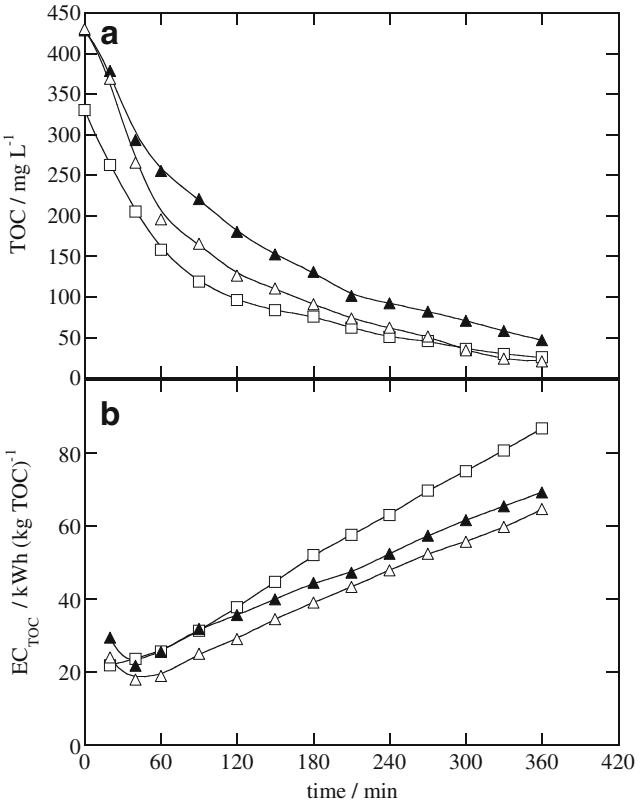

Fig. 14 Variation of **a** TOC and **b** energy consumption per unit TOC mass with electrolysis time for the SPEF treatment of 2.5 L of a simulated textile dyeing wastewater (330 mg L^{-1} TOC from additives) with 0.10 M Na_2SO_4 of pH 3.0 at 1.0 A, 35 °C, and liquid flow rate of 200 L h^{-1}. The solutions contained the following: *white square* 0.5 mM Fe^{2+}+0.1 mM Cu^{2+}, *black triangle* 0.5 mM Fe^{2+}+200 mg L^{-1} Disperse Blue 3, *white triangle* 0.5 mM Fe^{2+}+0.1 mM Cu^{2+}+200 mg L^{-1} Disperse Blue 3. Adapted from Salazar et al. (2012)

The study of the SPEF process has been lately extended to a 10-L pre-pilot plant, schematized in Fig. 15a (Isarain-Chávez et al. 2011). This plant has the same components as those shown in Fig. 14a, but with a reactor of 90.3 cm^2 electrode area coupled to a 1.57-L solar compound parabolic collector (CPC) as the photoreactor. The research was focused on the optimization of the SPEF treatment of the drug paracetamol using a Pt/ADE cell by response surface methodology (Almeida et al. 2011). The optimal variables were found to be 5 A, 0.4 mM Fe^{2+}, and pH 3.0 for 157 mg L^{-1} paracetamol with 0.05 M Na_2SO_4, yielding 75 % TOC reduction, 93 kWh(kg TOC)$^{-1}$ energy consumption, and 71 % current efficiency at 120 min. HPLC analysis of electrolyzed solutions allowed detecting hydroquinone and various benzoquinones as aromatic intermediates, which were removed by $^{\bullet}OH$, whereas maleic, fumaric, succinic, lactic, oxalic, formic, and oxamic acids were identified as carboxylic acids. Recently, the SPEF treatment of 297 mg L^{-1} of the azo dye Sunset Yellow FCF in 0.05 M Na_2SO_4 and 0.5 mM Fe^{2+} of pH 3.0 using the same system at 7 A demonstrated that total decolorization was feasible at 120 min and that approximately 94 % mineralization with 197 kWh(kg TOC)$^{-1}$ energy consumption was attained at 150 min (Moreira et al. 2013).

The SPEF degradation of 100 mg L^{-1} TOC of solutions with the beta-blockers atenolol, metoprolol tartrate, and propranolol hydrochloride in 0.10 M Na_2SO_4 with 0.5 mM Fe^{2+} at pH 3.0 was tested using single Pt/ADE and BDD/ADE cells and also their combination with a Pt/CF cell to enhance Fe^{2+} regeneration from Fe^{3+} reduction (Isarain-Chávez et al. 2011). Figure 15b shows a sketch of the combined BDD/ADE–Pt/CF cell. As an example, Fig. 16a highlights for a 0.246-mM metoprolol tartrate solution the superiority of combined cells over single cells, BDD over Pt, and SPEF over EF regarding TOC abatement. This can be explained by the greater production of $^{\bullet}OH$ from Fenton's reaction in the combined cells, the higher oxidizing power of BDD($^{\bullet}OH$), and the photolytic action of sunlight in SPEF, as easily deduced from the pseudo-first-order decay kinetics shown in Fig. 16b. Nevertheless, the Pt/ADE–Pt/CF cell gave the lowest energy consumption of 80 kWh(kg TOC)$^{-1}$ for 88–93 % mineralization, being the most viable system for industrial application.

Photoelectrocatalysis

The PEC method relies on the synergy between electrochemistry and photocatalysis to provide much greater efficiency for wastewater remediation. Traditional photocatalysis has been extensively developed using the nanocrystalline anatase form of TiO_2 for light-induced oxidation of organic pollutants in waters (Brillas et al. 2009; Daghrir et al. 2012a; Georgieva et al. 2012). This semiconductor material possesses very attractive properties such as low cost, low toxicity, and a wide band gap of 3.2 eV, which results in good stability and prevents photocorrosion. The irradiation of anatase TiO_2 nanoparticles, either in colloidal suspension or deposited as a thin film on Ti, by UV photons of sufficient energy (λ<380 nm) promotes an electron from the valence band to the conduction band (e^-_{CB}), generating a positively charged vacancy or hole (h^+_{VB}) as follows:

$$TiO_2 + h\nu \rightarrow e^-_{CB} + h^+_{VB} \quad (58)$$

Organics can then be directly oxidized by the hole or by heterogeneous $^{\bullet}OH$ formed from the reaction between the photogenerated vacancy and adsorbed water:

$$h^+_{VB} + H_2O \rightarrow {}^{\bullet}OH + H^+ \quad (59)$$

In addition, other weaker reactive oxygen species (ROS; superoxide radical ion $O_2^{-\bullet}$, $HO_2^{\bullet}$, and H_2O_2) and more $^{\bullet}OH$

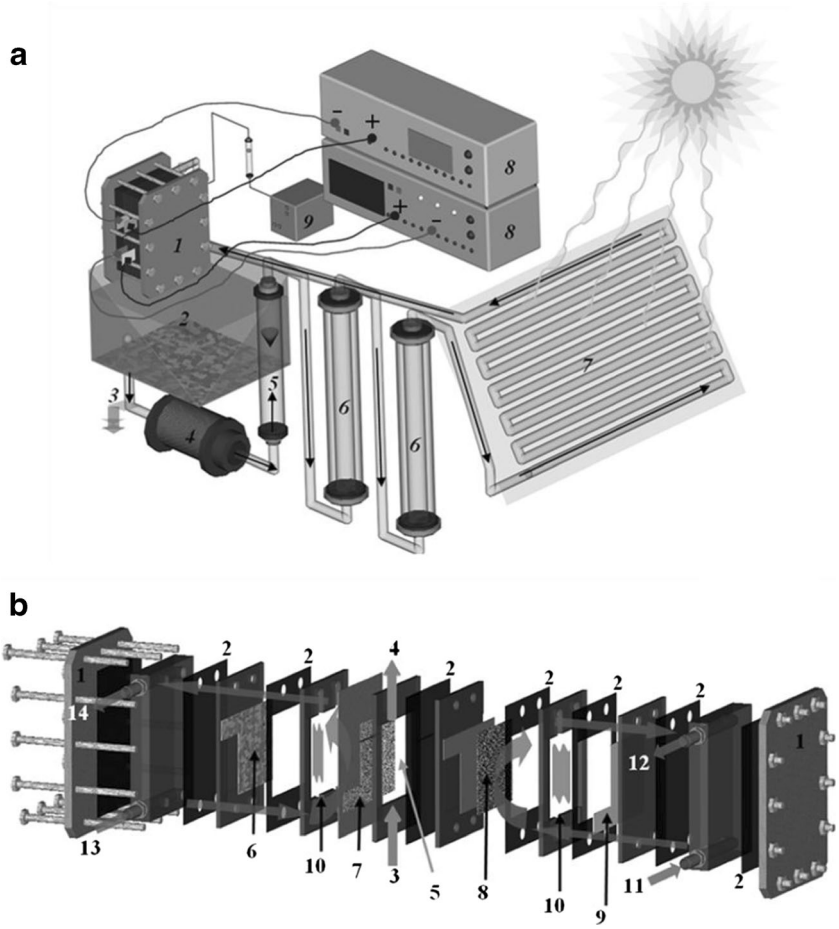

Fig. 15 **a** Experimental setup of a 10-L recirculation pre-pilot plant for the SPEF treatment of organic pollutants. *1* Flow electrochemical cell, *2* reservoir, *3* sampling, *4* peristaltic pump, *5* flow meter, *6* heat exchanger, *7* solar CPC (photoreactor), *8* power supply, *9* air pump. **b** Scheme of a combined filter–press electrochemical cell. *1* End plate, *2* gasket, *3* air inlet, *4* air outlet, *5* air chamber, *6* 90 cm^2 BDD anode, *7* 90 cm^2 ADE cathode, *8* 90 cm^2 CF cathode, *9* 90 cm^2 Pt anode, *10* liquid compartment, *11* liquid inlet in the cell, *12* liquid outlet of the Pt/CF pair connected to 13, *13* liquid inlet in the BDD/ADE pair, *14* liquid outlet of the cell. Adapted from Isarain-Chavez et al. (2011)

can be produced from the photoinduced electron based on the following reactions:

$$e^-_{CB} + O_2 \rightarrow O_2^{-\bullet} \quad (60)$$

$$O_2^{-\bullet} + H^+ \rightarrow HO_2^{\bullet} \quad (61)$$

$$2\ HO_2^{\bullet} \rightarrow H_2O_2 + O_2 \quad (62)$$

$$H_2O_2 + O_2^{-\bullet} \rightarrow {}^{\bullet}OH + OH^- + O_2 \quad (63)$$

The significant decrease in efficiency results from the recombination of photoinduced electrons with either unreacted holes or adsorbed $^{\bullet}OH$:

$$e^-_{CB} + h^+_{VB} \rightarrow TiO_2 + \text{heat} \quad (64)$$

$$e^-_{CB} + {}^{\bullet}OH \rightarrow OH^- \quad (65)$$

By contrast, the PEC method consists in the application of either a constant current or a constant bias anodic potential (E_{anod}) to a semiconductor-based thin film anode subjected to UV illumination for the continuous extraction of photoinduced electrons by an external electrical circuit. This minimizes the extent of Eqs. 60, 61, 62, 63, 64, and 65 and favors the generation of a higher quantity of holes from Eq. 58 and heterogeneous $^{\bullet}OH$ from Eq. 59, thereby largely enhancing organics oxidation and the process efficiency in comparison to photocatalysis (Daghrir et al. 2012a; Georgieva et al. 2012).

The electrolytic cells used in PEC are stirred tanks or flow reactors that permit the passage of UV light directly to the solution or through a quartz window to reach the exposed surface of the photoanode with the minimum loss of incident irradiation. Figure 17 shows a scheme of a stirred tank reactor directly illuminated with a solar simulator for the solar PEC (i.e., SPEC) treatment of bisphenol A (Frontistis et al. 2011). The most typical photoanodes are based on TiO_2 coatings (Osugi et al. 2008; Liu et al. 2009; Zhang et al. 2010; Frontistis et al. 2011; Xin et al. 2011; Daghrir et al. 2012b; Garcia-Segura et al. 2013), although other materials including ZnO (Zhang et al. 2008; Sapkal et al. 2012), Bi_2MoO_6-BDD (Zhao et al. 2009), WO_3 (Nissen et al. 2009; Scott-Emuakpor et al. 2012), and BiO_x–TiO_2 (Park et al. 2012) have also been utilized.

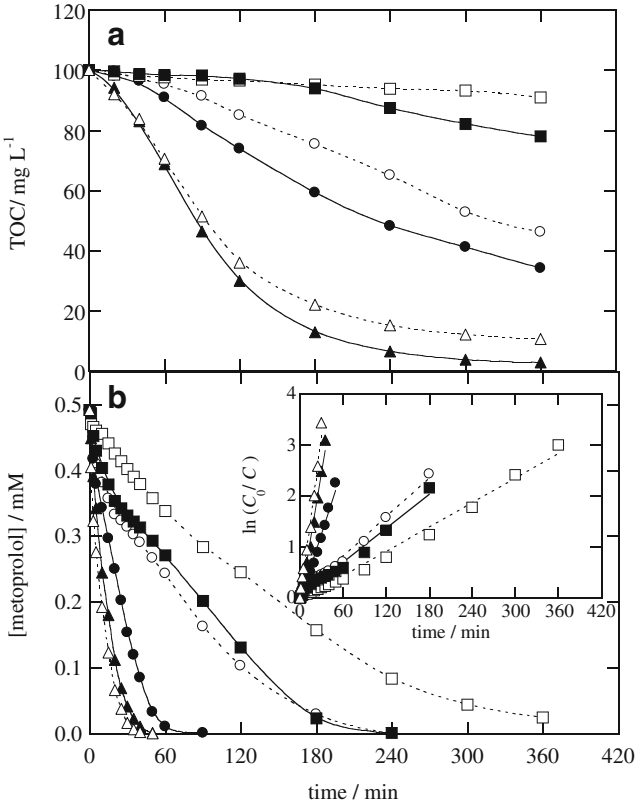

Fig. 16 **a** TOC removal with electrolysis time for the EF and SPEF treatments of 10 L of 0.246 mM metoprolol tartrate in 0.10 M Na_2SO_4 with 0.5 mM Fe^{2+} at pH 3.0 and 35 °C in the pre-pilot plant of Fig. 15a with single and combined cells. **b** Decay of 0.492 mM metoprolol under the same conditions. The *inset panel* shows the kinetic analysis assuming a pseudo-first-order reaction for the pharmaceutical. *White square* EF in Pt/ADE cell at 3.0 A, *black square* EF in Pt/ADE–Pt/CF cell at 3.0–0.4 A, *white circle* EF in BDD/ADE cell at 3.0 A, *black circle* EF in BDD/ADE–Pt/CF cell at 3.0–0.4 A, *white triangle* SPEF in Pt/ADE–Pt/CF cell at 3.0–0.4 A, *black triangle* SPEF in BDD/ADE–Pt/CF cell at 3.0–0.4 A. Adapted from Isarain-Chavez et al. (2011)

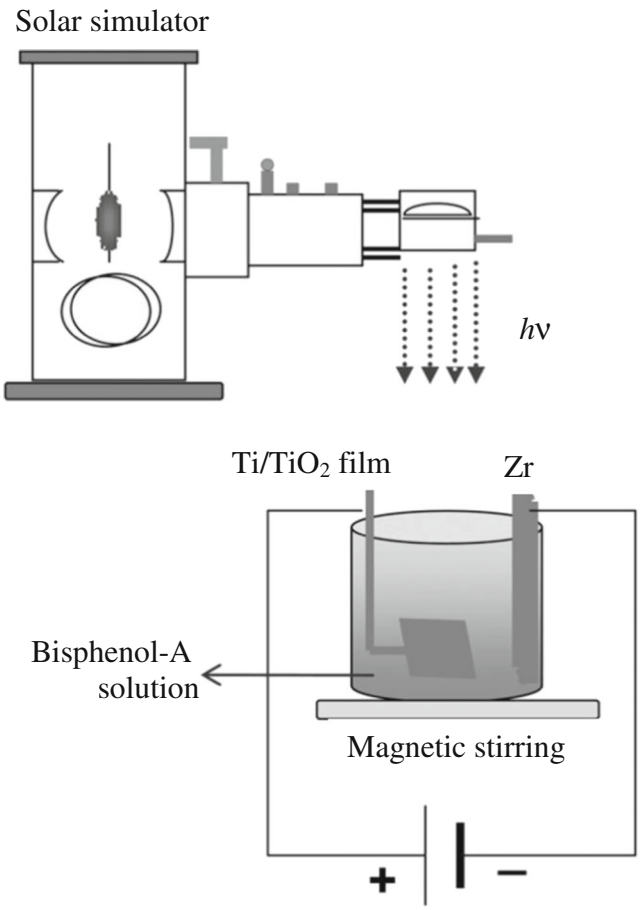

Fig. 17 Experimental setup for the SPEC treatment of 60 mL of a bisphenol A solution. A solar simulator with a 150-W Xe lamp and current density in the range of 0.02–0.32 mA cm^{-2} were employed. Adapted from Frontistis et al. (2011)

The efficient degradation of several dyes by PEC with a TiO_2 photoanode has been well proven. Osugi et al. (2008) used Ti/TiO_2 nanotubular array electrodes and nanoporous Ti/TiO_2 electrodes prepared by the sol–gel method to treat 0.05 mM of Disperse Red 1, Disperse Orange 1, and Disperse Red 13 and/or 80 mg L^{-1} of Emulsogen anionic surfactant in 0.10 M Na_2SO_4 under UV light and E_{anod}=+1.0 V/Ag/AgCl. After 60 min, all dye solutions were completely decolorized using the former electrode, with an apparent rate constant approximately two to three times higher than using the other electrode. TOC was removed approximately 70 % after 3 h with total disappearance of peaks related to aromatics detected in HPLC chromatograms. Zhang et al. (2010) prepared a Ti/TiO_2 nanotubular disk electrode of 38 cm^2 area to completely decolorize 36 mL of 50 mg L^{-1} of methyl orange dye in 0.01 M Na_2SO_4 after 3 h of illumination with a 15-W UVC lamp at E_{anod}=+0.75 V. Recently, a highly stable 3-cm^2 TiO_2 coating composed of 29 % rutile, 9 % anatase, and 62 % of Ti_7O_{13} on stainless steel support was prepared by atmospheric plasma spray (Garcia-Segura et al. 2013). This novel photoanode was coupled with a 3-cm^2 ADE in a stirred tank reactor to decolorize 100 mL of Acid Orange 7 azo dye solutions in 0.05 M Na_2SO_4 under direct sunlight. This SPEC process was based on the contribution of both solar photocatalysis and AO, owing to the larger production of $^{\bullet}OH$ from the higher amounts of holes that can be separated from photoinduced electrons. The best operation variables for SPEC were 15 mg L^{-1} dye, pH 7.0, and anodic current density of 1.0 mA cm^{-2}, for which the dye disappeared in 100 min and the solution was totally decolorized in 120 min, although only 40 % mineralization was attained in 240 min. Phthalic, tartaric, succinic, acetic, and oxamic acids were detected as intermediates, with the release of NH_4^+ ions in larger proportion than NO_3^- ions.

Less is known about the PEC treatment of dyes using other kinds of photoanodes. ZnO nanorods embedded in highly ordered TiO_2 nanotube arrays of 1 cm^2 area, coupled with a Pt anode in a stirred tank reactor and illuminated with a 11-W UVC lamp were able to completely decolorize a 0.05-mM

methyl orange solution in 0.5 M Na_2SO_4 of pH 6.2 after 90 min of PEC at E_{anod}=+0.60 V/SCE (Zhang et al. 2008). By contrast, 93 % decolorization with 69 % COD reduction has been reported after 3 h of PEC degradation of a textile industrial effluent under recirculation in a single tank reactor equipped with an UV-illuminated transparent ZnO thin film deposited onto a substrate of fluorine-doped tin oxide glass by the spray pyrolysis technique (Sapkal et al. 2012).

The viability of PEC for the destruction of pharmaceuticals has been checked by several authors (Liu et al. 2009; Zhao et al. 2009; Bai et al. 2010; Daghrir et al. 2012b; Fang et al. 2013). Thus, Liu et al. (2009) treated synthetic tetracycline wastewaters with a TiO_2 nanotube arrays photoanode at E_{anod}=+0.50 V/SCE illuminated with a 4-W UVC lamp in a stirred undivided three-electrode rectangular quartz reactor. The tetracycline content was reduced by 81 % in PEC, whereas it only decayed by 2 % for AO, 16 % for direct photolysis, and 38 % for photocatalysis. More recently, this group developed a novel double thin-layer PEC reactor that increased the ratio of electrode area to solution volume, enhancing the mass transport and the photonic efficiency, so that, the degradation of tetracycline became much quicker (Bai et al. 2010). The same group also examined the SPEC degradation of ibuprofen and naproxen with an innovative porous Bi_2MoO_6 film deposited onto BDD, with 11 cm^2 area exposed to a 150-W Xe lamp to simulate sunlight and immersed into 60 mL of solution with 0.12 mg L^{-1} Na_2SO_4 filling a cylindrical quartz cell (Zhao et al. 2009). At E_{anod}=+2 V/SCE, 86 % decay for 10 mg L^{-1} ibuprofen with 72 % TOC removal was found for SPEC, values much higher than 64 and 42 % obtained for AO and 21 and 8 % for photocatalysis, respectively. The partial effectiveness of AO indicated the ability of Bi_2MoO_6 to generate ROS at the high applied E_{anod}. Recently, Daghrir et al. (2012b) reported the efficient PEC degradation of 1 L of 25 μg L^{-1} chlortetracycline hydrochloride in 0.05 M Na_2SO_4 solution of pH near 6 using a 110-cm^2 Ti/TiO_2 nanocrystalline anode in a two-electrode cell under UVC illumination. After 120 min of electrolysis at anodic current density of 390 mA, the initial drug concentration diminished up to 98 %, while TOC and total nitrogen were reduced by 67 and 69 %, respectively. Based on biotesting, these authors demonstrated that the treated effluent was not toxic compared with the untreated effluent. It has also been described that the COD and color of 500 mL of a real pharmaceutical wastewater with the addition of NaCl were reduced by 93 and 78 %, respectively, by PEC in a quartz cell equipped with a 10-cm^2 Ni/TiO_2 photoanode exposed to a 250-W high-pressure mercury lamp and a 10-cm^2 multiwalled CNT air cathode (Fang et al. 2013).

Other compounds like bisphenol A (Frontistis et al. 2011) and the herbicide alachlor (Xin et al. 2011) have also been degraded by SPEC with a Ti/TiO_2 photoanode. Using the photoelectrochemical cell shown in Fig. 17, Frontistis et al. (2011) degraded 60 mL of 120–820 μg L^{-1} bisphenol A at pH between 1.0 and 7.5 and anodic current density from 0.02 to 0.32 mA cm^{-2}. The reaction was favored up to 0.04 mA cm^{-2} and at low substrate concentrations, but was hindered by the presence of residual organic matter and radical scavengers like bicarbonates. As expected, SPEC was much more efficient than pure TiO_2 photocatalysis or AO. The same behavior was reported by Xin et al. (2011) for alachlor treatment, showing a higher performance using a nanotube-shaped Ti/TiO_2 photoelectrode compared with a wormhole-shaped Ti/TiO_2 photoelectrode.

Finally, the PEC performance of innovative photoanodes such as WO_3 and Ti/BiO_x–TiO_2 on other contaminants has been assessed. The WO_3 photoelectrode was exposed to visible light either in a reactor configuration that resembled a fuel cell with a Nafion 115 membrane and a Pt/carbon printed onto Teflon/carbon as cathode (Scott-Emuakpor et al. 2012) or in an H-cell where the photoanode and the Pt gauze cathode were separated by an agar–salt bridge (Nissen et al. 2009). In both systems, very slow removal of 0.25 mM of 2,4-DCP, along with a large formation of chloroderivatives, was obtained after 24 h of PEC as a result of the very little current which was able to circulate through the external circuit, causing a large recombination of photogenerated holes and electrons and favoring oxidation with the generated ClO^- ion. In contrast, the BiO_x–TiO_2 acted as an actual photoelectrode and showed a much higher oxidation ability of organics (Park et al. 2012). When this anode was exposed to a 450-W Hg–Xe lamp and coupled with a stainless steel cathode, both of 50 cm^2 area, in a stirred tank reactor with 1.5 L of 1 mM phenol and 0.05 mM NaCl at constant voltage >1 V, the anodic phenol oxidation rate and the cathodic H_2 production rate were enhanced by factors of 4 and 3, respectively, as compared with the sum of light irradiation and direct electrolysis.

Hybrid combinations of PEF and PEC

The decolorization of several dyes has been enhanced by combining PEF and TiO_2 photocatalysis (TiO_2/UV), as reported by Khataee et al. (2010, 2012), who optimized the experimental conditions using response surface methodology. These authors utilized open, undivided, and cylindrical stirred tank reactors of 1 or 3 L capacity equipped with a Pt anode, a cathode composed of CNT immobilized onto a graphite surface (CNT/graphite) fed with air, a 6-W UVC lamp introduced into a quartz tube, and TiO_2 nanoparticles immobilized on paper or glass plates covering the inner surface of the cell. For the azo dye Acid Yellow 36 (Khataee et al. 2012), for example, the decolorization rate decreased in the sequence PEF-TiO_2/UV>PEF>EF>TiO_2/UV>UV photolysis. The optimum variables for the former combined process were 25 mg L^{-1} of dye, 0.15 mM Fe^{3+}, 127 min of treatment, and 115.6 mA, yielding a maximum color removal of 83 %. It is worth noting that the operation costs related to the use of the

UV lamp were as high as 16.5 kWh m^{-3}, whereas the electrical energy consumption was only 0.88 kWh m^{-3}.

By contrast, several attempts have also been made to enhance the oxidation ability of PEC by its coupling with EF, although more studies are needed to confirm the use of such combined processes. Xie and Li (2006) used the quartz reactor shown in Fig. 18a to study the removal of azo dye Orange G for 5 h by different methods. The cell was filled with 30 mL of a 0.1-mM solution of the dye containing 0.01 M Na_2SO_4 at pH 6.2, and an 8-W UVA lamp was used as light source. Figure 18b highlights that Orange G was not directly photolyzed under UVA irradiation, being slightly destroyed (approximately 3 %) by AO with a TiO_2/Pt cell at E_{anod}=+0.71 V/SCE and reaching 8 % by TiO_2 photocatalysis, as expected if small quantities of oxidizing species ($^{\bullet}OH$ and/or holes) are formed at the TiO_2 surface. The PEC process using the Pt/TiO_2 cell enhanced dye removal

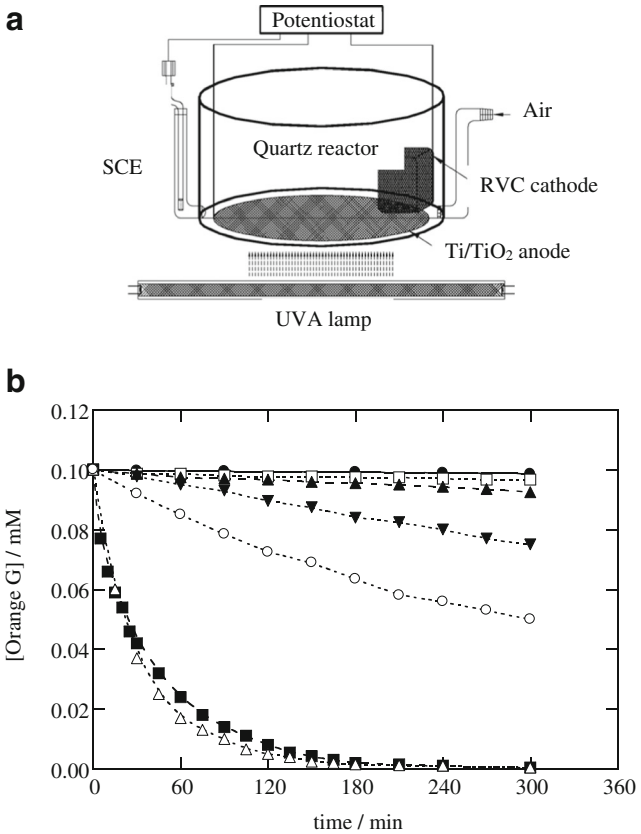

Fig. 18 **a** Experimental setup of the aerated three-electrode undivided quartz cell with 5 cm^2 electrodes used for the photo-assisted electrochemical oxidation of 30 mL of a 0.1-mM Orange G solution with an 8-W UVA lamp. In PEC, the bias potential applied to the Ti/TiO_2 anode was + 0.71 V/SCE, whereas an E_{cat} of −0.54 or −0.71 V/SCE was applied to the RVC for H_2O_2 electrogeneration. **b** Dye concentration decay from *black circle* direct photolysis, *white square* AO with a TiO_2/Pt cell, *black up-pointing triangle* TiO_2 photocatalysis, *black down-pointing triangle* PEC with a TiO_2/Pt cell, *white circle* PEC with a TiO_2/RVC cell, *black square* PEF with 17.6 mg L^{-1} Fe^{2+} at pH 3.0 with Fe/RVC cell, *white triangle* PEC coupled to EF with 17.2 mg L^{-1} Fe^{2+} at pH 3.0 using a TiO_2/RVC cell. Adapted from Xie and Li (2006)

to 25 % due to the photogeneration of more amounts of oxidizing holes. The oxidation ability of this technique increased to yield 50 % dye destruction when the Pt cathode was replaced by an RVC electrode at E_{cat}=−0.54 V/SCE, making possible dye oxidation with H_2O_2 produced from O_2 reduction. Interestingly, Orange G disappeared completely when applying PEF with an Fe/RVC cell using approximately 17 mg L^{-1} Fe^{2+}, pH 3.0, and E_{cat}=−0.71 V/SCE. Furthermore, the decolorization rate slightly increased if EF under the same conditions was coupled to PEC using a TiO_2/RVC cell, as a result of the additional formation of large amounts of homogeneous $^{\bullet}OH$ from Fenton's and/or photo-Fenton reaction. As a result, PEC coupled with EF provided the highest mineralization of 74 % in 5 h. Peralta-Hernández et al. (2006) also described a significant improvement in the decolorization efficiency and TOC removal by PEC coupled to EF in comparison to EF alone using a concentric annular undivided TiO_2/graphite cloth flow cell with a central 75 mW cm^{-2} UVA lamp in batch operation mode.

Prospects

It is evident that intensification in most novel research pathways in the environmental electrochemistry field will eventually yield positive results regarding the enhancement of photoelectrochemical processes as well. In this sense, attention to advanced electrodes and reactors, along with process modeling, can lead to a comprehensive expansion of such processes into all areas of environmental preservation, including remediation of contaminated waters, gaseous streams, and soils. There exists an undoubtedly optimistic background because significant progress has been evidenced from the development of novel electrodes and membranes and the optimization of the reactor setup, including, for example, the development of more efficient multiple-phase oxidation and three-dimensional electrode reactors. However, a critical analysis of the immediate challenges of the photoelectrochemical processes for the treatment of organic pollutants in waters has to focus on the particularities of PEC and SPEF, given their preponderance.

The use of new advanced anode materials in PEC, such as oxide semiconductors in the form of nanotubes/nanorods/nanowires including those based on TiO_2, has shown an increasing generated photocurrent. Also, the preparation of electrodeposited coatings of pure, doped, and composite photoelectrocatalytic materials should be further explored, given the very interesting resulting physicochemical properties and the excellent surface finishing upon use of this manufacturing methodology. Unfortunately, to be realistic, poor results concerning mineralization have been reported so far by means of PEC. TOC and COD removals are usually lower than 100 %, as discussed previously, and the abatements are always slow as a result of the mass transport limitations

that are inherent to an electrode process such as this one. Indeed, this is common major drawback, also found in electro-oxidation, but in that case, the alternative mediated oxidation by generation of other oxidants such as active chlorine or peroxo salts (e.g., persulfates, percarbonates, and perphosphates) at very powerful anodes like BDD has allowed the enthusiastic rebirth and promising development of new applications of that technology, as for example in water disinfection systems. Of course, new advances on PEC are closely related to the progress in the field of photocatalysis, particularly concerning the ability of materials engineering to propose more efficient photocatalysts that show a higher absorption in the visible range of the solar spectrum. As an immediate consequence of such expected developments and considering the previously exposed results on PEC, we suggest the alternative combination of SPEC with SPEF, a hybrid system that has not been tested yet, since it would definitely be much more economical than the PEC combinations assessed in recent years.

By contrast, SPEF is sufficiently promising by itself, and future modifications point out to the economical aspects. Some of us are involved in conceiving sunlight-driven systems based on solar panels and photovoltaic energy as a cheap source of electrical power. As commented, work conducted at pre-pilot plants under laboratory conditions has confirmed the much superior economic viability of SPEF over other electrochemical treatments such as AO, EF, and PEF, especially for the treatment of specific effluents with a notable acidity that allow the straightforward application of Fenton's reaction. A joint project between the Universitat de Barcelona and the Plataforma Solar de Almería (PSA, Spain), which is the largest European facility for research on solar technologies, is seeking the scale-up of the SPEF technology. Hopefully, coupling with other sunlight-assisted processes carried out within that facility will lead to an integral, robust technology which can catch the attention of private entrepreneurs and the public sector.

Sonoelectrochemical processes

As deduced from comments in the "Activation by ultrasound irradiation" section, US is able to produce highly reactive radicals from water as well as the pyrolysis of organic pollutants contained in such matrices. However, its oxidation ability is rather low and, consequently, it is usually combined with other oxidants like H_2O_2, O_2, UV, and Fenton's reagent for water remediation (Oturan et al. 2008; Garbellini et al. 2008; González-García et al. 2010; Garbellini 2012). The study of the combination of US and electrode processes and the application of sonoelectrochemical technology to the combustion of organic compounds are current active research fields (Garbellini et al. 2008; Garbellini 2012). This section describes the characteristics of sonoelectrolysis and SEF, which are the most important sonoelectrochemical processes used to decontaminate wastewaters.

Sonoelectrolysis

The combination of an US field with electrochemical oxidation can result in a powerful method for pollutant degradation. US can improve the electrochemical degradation of pollutants by chemical and physical mechanisms (Garbellini 2012). The chemical mechanism is found at high frequency and involves the homolytic fragmentation of H_2O and dissolved O_2 to yield different ROS ($^{\bullet}OH$, $HO_2^{\bullet}$, and $^{\bullet}O$). The physical mechanism is so-called sonication and consists in the production of cavitation microbubbles which grow and collapse, originating great breaking forces with extremely high temperatures (up to 6,000 K) and pressures (of the order of 10^4 kPa). Under these conditions, organics can be directly pyrolyzed and the sonolysis of water can be expressed in Eq. 66, where))) denotes US, while $^{\bullet}OH$ thus generated accelerates the organics oxidation:

$$H_2O +))) \rightarrow {}^{\bullet}OH + {}^{\bullet}H \quad (66)$$

In addition, the strong cavitational collapse near the electrode surface enhances the mass transport of the electroactive species as well as the cleaning of the electrodes' surfaces by dissolving or pitting the inhibiting layers (Garbellini et al. 2008; Garbellini 2012). All these phenomena largely improve the destruction rate of organics, eventually favoring the mineralization process in sonoelectrolysis.

Several experimental setups have been conceived for sonoelectrochemical experiments, as follows: (i) immersion of the electrochemical cell inside an US bath, (ii) coupling of the electrolytic cell with the ultrasonic tip through a glass wall or filled liquid chambers, (iii) use of a sonoelectrochemical cell where the electrodes and the US tip are directly dipped into the working solution, which turns out to be the most used arrangement, and (iv) the simultaneous use of the US tip as US emitter and as electrode (González-García et al. 2010). Figure 19 shows an image of an US tip near a BDD electrode in a sonoelectrolytic cell (Garbellini 2012). The vast majority of research in sonoelectrolysis has been carried out at laboratory scale with individually designed systems based on powerful US horns dipped into traditional glass electrochemical vessels. This procedure is very expensive and has evidenced some drawbacks related to reproducibility, scale-up, and design aspects which have slowed down its further development.

The benefits derived from using sonoelectrolysis for the removal of dyes has been explored by several authors. Lorimer et al. (2001) treated solutions of 500 mL of approximately 20 mg L^{-1} of basic dyes like Yoracyl Brilliant Red, Astrazon Golden Yellow GL, Maxilon Blue 5G, and Astrazon

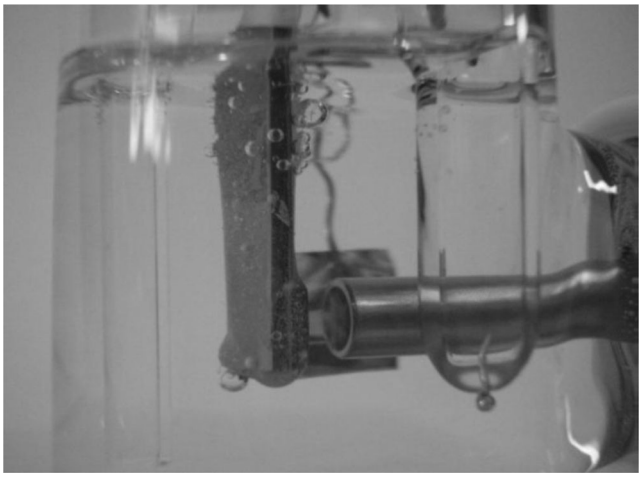

Fig. 19 US tip in front of a BDD anode (distance=5 mm) in a sonoelectrochemical reactor for organic pollutant degradation. Adapted from Garbellini (2012)

Red GTLN by low-power, high-frequency US (1.1 W cm^{-2}; 510 kHz), and the acidic dye Sandolan Yellow by high-power, low-frequency US (20–100 W cm^{-2}; 20 kHz). US alone decolorized the basic dyes due to the attack of H_2O_2 formed from the dimerization of generated $^{\bullet}OH$, but it was unable to destroy the acidic dye. Subsequently, in sonoelectrolysis tests, a tank reactor containing either a 13.5-cm^2 carbon or a 2-cm^2 Pt anode was placed inside the US bath. All dyes were efficiently removed by electrolysis and sonoelectrolysis in an aqueous chloride electrolyte owing to their reaction with ClO^- ion formed from Cl^- AO. Comparative trials showed that the oxidation ability of processes decreased in the sequence: sonoelectrolysis>electrolysis>sonolysis. The decolorization rate increased with increasing current from 50 to 300 mA, chloride concentration (up to 0.5 M), and/or US power. The best performances were attained using the low frequency of 20 kHz, being related to the cavitation effects of US that promotes degassing at the electrode surface, improves the mass transport of species across the diffusion layer, and favors the continuous cleaning and activation of the electrode surfaces. More recently, it has been described that, in a similar sonoelectrolytic system composed of a PbO_2/stainless steel cell submitted to an US source of 300 W and 8 kHz, a solution of 1 L of 50 mg L^{-1} of unhydrolyzed Reactive Blue 19 dye at pH 8.0 attained 90 % color removal and 56 % TOC removal after 120 min of sonolysis alone, whereas the use of sonoelectrolysis accelerated the treatment and total decolorization was achieved at 30 min under a cell voltage of 10 V (Siddique et al. 2011). Lately, a novel Ti/SnO_2–Sb_2O_3/PTFE–La-Ce-β-PbO_2 anode of high density and preferred crystalline structure has been proposed to improve the mass transport and mineralization of the cationic dye Gold Yellow X-GL under sonoelectrolysis (Dai et al. 2012).

Sonoelectrolysis has also been applied to the treatment of waters contaminated with very refractory compounds like trichloroacetic acid and perchloroethylene. The degradation of trichloroacetic acid was examined by Esclapez et al. (2010), who scaled up to a pre-pilot flow plant equipped with a divided Ti/Pt reactor and an US transducer of 3.8 W cm^{-2} under the recirculation of an anolyte of 1 L of 3 mM substrate with 0.010 M Na_2SO_4 at 100 L h^{-1}. Although 97 % of fractional conversion of trichloroacetic acid could be obtained in this system, the degradation efficiency was only of 26 % and the current efficiency was as low as 8 %. Better results were reported by the same Spanish group for perchloroethylene (Sáez et al. 2010b, 2011). Preliminary trials were made in a PbO_2/Pb undivided tank reactor of 12 cm^2 electrode area equipped with an US transducer supplying up to 7.52 W cm^{-2} and 20 kHz. The treatment of 200 mL of 0.452 mM perchloroethylene in 0.05 M Na_2SO_4 of pH 6.0 at 3.5 mA cm^{-2} gave 100 % degradation efficiency and approximately 55 % of current efficiency, regardless of the power used. The complete removal of this substrate in the absence of background electrolyte was also found, surprisingly with even greater current efficiency than in the presence of 0.05 M Na_2SO_4. However, the energy cost increased considerably due to the much higher cell voltage applied, which is a drawback for sonoelectrolytic treatment of wastewaters with low salt concentrations.

The effect of US on the electrochemical combustion of organics with a BDD anode has been recently explored. The cleaning of the electrode surface and enhancement of mass transport were evaluated by performing potentiostatic electrolyses of 90 mL of 0.05 mM PCP as anolyte in an H-cell using a 0.42-cm^2 BDD anode and an US tip placed at 7 cm in front of it (Fig. 19) and supplying a radiation of 14 W and 20 kHz (Garbellini et al. 2010). After 270 min at E_{anod}=+3.0 V vs. Ag/AgCl, the substrate was removed by 20 % for sonolysis, 71 % for direct electrolysis, and 83 % for sonoelectrolysis. The higher removal achieved in the latter system was explained by the increase in mass transport, minimization of the electrode fouling, and the combined generation of $^{\bullet}OH$ by both US and polarized BDD surface. Similar trends for these processes have been described for the mineralization of the herbicide diuron in aqueous medium (Bringas et al. 2011) and the antibiotic triclosan in methanol/water or methanol solutions (Martín de Vidales et al. 2012). In the latter case, sonoelectrolysis was more efficient in sulfate than in chloride medium, and the main intermediates detected by HPLC were catechol, chlorohydroquinone, 4-chlorocatechol, acetic acid, and dichloroacetic acid due to the oxidative action of generated $^{\bullet}OH$ mainly at the BDD anode.

An interesting work dealing with the electrosynthesis of H_2O_2 from cathodic O_2 reduction in the absence and presence of US was reported by González-García et al. (2007). These authors used a vertical two-compartment three-electrode cell equipped with an RVC cathode of 30 mm×40 mm×10 mm in dimension, an SCE reference electrode, and an Ni gauze anode with a cationic exchanger membrane as separator. The reactor was subjected to US provided by a horn of 1,000 W

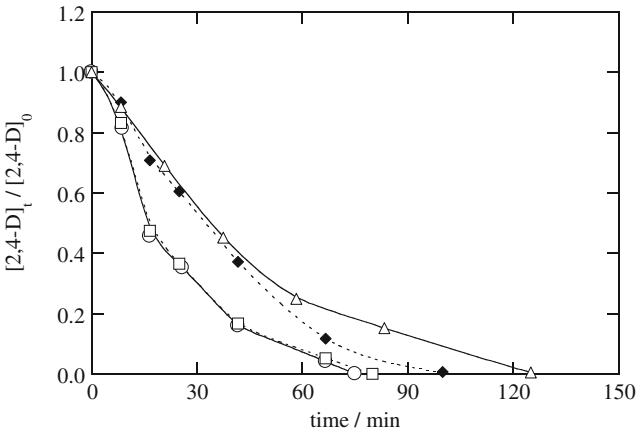

Fig. 20 Decay of 2,4-D concentration with time during the treatment of 250 mL of 1 mM herbicide in the presence of 0.1 mM Fe^{3+} as catalyst, at 200 mA, pH 3.0, and room temperature in a Pt/CF cell. SEF process with low-frequency US of 28 kHz and at output power of *white circle* 20 W, *white square* 60 W, *white triangle* 80 W, *black diamond* EF process alone. Adapted from Oturan et al. (2008)

and 20 kHz. The catholyte was 1.25 L of an O_2-saturated NaOH solution of pH 13 or borate buffer of pH 10.0 under recirculation at a flow rate of 70 or 300 L h^{-1}. The application of US at E_{cat}=−1.0 V/SCE enhanced both the H_2O_2 concentration and the current efficiency of the process, preferentially at the smaller flow rate. For example, current efficiencies of approximately 60 % were reached under the application of US at pH 10 and 70 L h^{-1}, conditions at which silent electrosynthesis had a current efficiency ≤20 %. This improvement was related to an enhanced mass transport of dissolved O_2 under US.

Sonoelectro-Fenton

The SEF process consists in the application of an US radiation to an acidic solution under EF conditions. It was proposed by Oturan et al. (2008), who demonstrated the benefits of this novel procedure for the degradation of herbicides 2,4-D and 4,6-dinitro-*o*-cresol using an undivided Pt/CF tank reactor with a ceramic piezoelectric transducer placed on its base to supply energies of 20, 60, and 80 W at a low frequency of 28 kHz. Figure 20 exemplifies the decay found for 2,4-D concentration in the absence and presence of US. The SEF process enhanced the destruction of this compound compared with EF for the lower energies of 20 and 60 W. This was ascribed to the mass transfer enhancement of O_2 to the electrode by sonication, which produced more H_2O_2 and accelerated the $^{\bullet}OH$ generation from Fenton's reaction, then reacting more rapidly with the herbicide. In contrast, the application of the higher US energy of 80 W significantly inhibited the SEF process probably because it caused the depletion of dissolved O_2 with the consequent decrease of H_2O_2 accumulation and $^{\bullet}OH$ generation required for the EF process.

More recently, the superiority of SEF over EF and chemical Fenton was demonstrated for the treatment of the cationic dyes Red X-GRL (Li et al. 2010) and Azure B (Martínez and Uribe 2012). An air-saturated solution of 1 L of 37.5 mg L^{-1} of the former dye with 0.05 M Na_2SO_4 and 5 mM Fe^{2+} of pH 3.0 in an undivided tank reactor with a Ti/RuO_2 anode and an activated carbon fiber cathode, each of 100 mm×90 mm area, was degraded by EF at 8.9 mA cm^{-2}. Comparative SEF trials were made using an US system of

Table 4 Main advantages and drawbacks of the EAOPs reviewed

Technology	Advantages	Drawbacks
Anodic oxidation	Treatment of large volumes (need of large anodes or cell stacks)	Electrode fouling
		Expensive, high O_2 overpotential anodes
	Very large percentages of organic matter degradation	Attention to halogenated by-products
	No pH restrictions	Usually work in batch mode
Fenton-based processes	Treatment of large volumes (need of large electrodes or cell stacks)	Need of pH regulation (pH near 3.0) and neutralization
		Quick and very large percentages of organic matter removal
	Degradation (more remarkable under sunlight irradiation)	Sludge formation
	Cathodic generation of H_2O_2	Attention to halogenated by-products
		Usually work in batch mode
Photoelectrocatalysis	Small bias potential required	High cost of UV lamps usage
	Slow but large percentages of organic matter degradation	Particular reactor configuration with photoactive anodes and quartz glass
	Immobilized photocatalyst (no need of separation filtration after treatment)	Attention to halogenated by-products
		Usually work in batch mode
Sonoelectrochemistry	Large enhancement of the mass transport of reactants toward/from the electrodes	High cost of US horns and usage
	Promotion of degassing at the electrode surfaces	Difficult system scale-up
	Prevention of electrode fouling	Usually work in batch mode

20 kHz and energies of 80, 120, and 160 W with the horn dipped into the solution at 20 mm of its surface and placed between the electrodes. The dye was always completely decolorized in 180 min, although color removal was enhanced by SEF, where it increased as US energy increased. A similar trend was found for TOC decay, which increased from 75 % in EF to 83 % in SEF at 160 W. For 0.5 mM Azure B, it was found that the rate constant for its decay in SEF by applying E_{cat}=−0.7 V/SCE to an RVC cathode under US of 91 W and 24 kHz was tenfold that of direct sonolysis and twofold that of the one obtained by chemical Fenton under silent conditions. Accordingly, COD was abated 68 % in 60 min by Fenton, whereas a much large value of up to 85 % was obtained by SEF.

Prospects

Sonochemistry is an emerging green technology in a large variety of research fields. Particularly, the application of sonoelectrochemical processes to the activation of radicals in electrolytic devices seems to gain a progressive acceptance among the scientific community, but for the moment, a significant percentage of works have been performed at the laboratory scale. It certainly accelerates the degradation of contaminants found in the liquid phase due to various simultaneous phenomena that take place, although a major detrimental factor is the high cost due to the inefficient use of energy. At present, most of the energy applied is not useful for oxidation but is dispersed as mechanical energy and heat, which could be ameliorated with an optimized design of the sonoelectrolytic reactors. Indeed, this could be a hot topic in future years to implement all the beneficial characteristics of acoustic cavitation in water treatment, and papers on modeling can be found lately. It has also been demonstrated that a very high US power is not required, which can then motivate the use of low-power pulse waves entailing a much affordable treatment.

Coupling with other processes may give rise to a more efficient decontamination such as in electro-oxidation with BDD or in sonophotoelectrocatalysis recently proposed. Nevertheless, the combination with bulk oxidation processes such as those based on Fenton's reaction is the most adequate target, considering the mechanisms that become activated in the presence of ultrasonic waves. By contrast, SE can allow the recovery of some priced pollutants, as in the case of metals. It is also known that ultrasonic cleaning technology is generally used as ultrasonic baths, and thus, cavitation may also prevent electrode fouling. An immediate advantage of those systems is related to preventing biofouling typically encountered in wastewater treatment facilities. Finally, related to this, US technology is currently under investigation for the inactivation of microorganisms such as bacteria and virus, therefore becoming an interesting hybrid technology for carrying out water disinfection.

Conclusion

All the work performed in the fields of research, development, and manufacturing has shown that the EAOPs technology has a huge potential for water purification and treatment in general. A comparison between all the technologies reviewed in this paper regarding their advantages and drawbacks is shown in Table 4. From our point of view, two main challenges should be prioritized, as follows: (i) the cut in electrode prices, particularly BDD, and (ii) the use of renewable energy sources to power the processes, thus enhancing the sustainability of all these EAOPs.

References

Abdessalem AK, Oturan N, Bellakhal N, Dachraoui M, Oturan MA (2008) Experimental design methodology applied to electro-Fenton treatment for degradation of herbicide chlortoluron. Appl Catal B Environ 78:334–341

Almeida LC, Garcia-Segura S, Bocchi N, Brillas E (2011) Solar photoelectro-Fenton degradation of paracetamol using a flow plant with a Pt/air-diffusion cell coupled with a compound parabolic collector: process optimization by response surface methodology. Appl Catal B Environ 103:21–30

Alverez-Gallegos A, Pletcher D (1999) The removal of low level organics via hydrogen peroxide formed in a reticulated vitreous carbon cathode cell. Part 2: the removal of phenols and related compounds from aqueous effluents. Electrochim Acta 44:2483–2492

Anglada Á, Urtiaga A, Ortiz I (2009) Contributions of electrochemical oxidation to waste-water treatment: fundamentals and review of applications. J Chem Technol Biotechnol 84:1747–1755

Anglada Á, Urtiaga AM, Ortiz I (2010) Laboratory and pilot plant scale study on the electrochemical oxidation of landfill leachate. J Hazard Mater 181:729–735

Anglada Á, Urtiaga A, Ortiz I, Mantzavinos D, Diamadopoulos E (2011) Boron-doped diamond anodic treatment of landfill leachate: evaluation of operating variables and formation of oxidation by-products. Water Res 45:828–838

Bai J, Liu Y, Li J, Zhou B, Zheng Q, Cai W (2010) A novel thin-layer photoelectrocatalytic (PEC) reactor with double-faced titania nanotube arrays electrode for effective degradation of tetracycline. Appl Catal B Environ 98:154–160

Balci B, Oturan MA, Oturan N, Sirés I (2009) Decontamination of aqueous glyphosate, (aminomethyl)phosphonic acid, and glufosinate solutions by electro-Fenton-like process with Mn^{2+} as the catalyst. J Agric Food Chem 57:4888–4894

Bautista P, Mohedano A, Casas J, Zazo J, Rodriguez J (2008) An overview of the application of Fenton oxidation to industrial wastewaters treatment. J Chem Technol Biotechnol 83:1323–1338

Bellakhal N, Oturan MA, Oturan N, Dachraoui M (2006) Olive oil mill wastewater treatment by the electro-Fenton process. Environ Chem 3:345–349

Bergmann MEH (2010) In: Comninellis C, Chen G (eds) Electrochemistry for the environment. Springer Science, New York, pp 163–204

Bergmann H, Iourtchouk T, Schöps K, Bouzek K (2002) New UV irradiation and direct electrolysis—promising methods for water disinfection. Chem Eng J 85:111–117

Bolyard M, Fair PS, Hautman DP (1992) Occurrence of chlorate in hypochlorite solutions used for drinking water disinfection. Environ Sci Technol 26:1663–1665

Borràs N, Arias C, Oliver R, Brillas E (2013) Anodic oxidation, electro-Fenton and photoelectro-Fenton degradation of cyanazine using a boron-doped diamond anode and an oxygen-diffusion cathode. J Electroanal Chem 689:158–167

Bouafia-Chergui S, Oturan N, Khalaf H, Oturan MA (2010) Parametric study on the effect of the ratios $[H_2O_2]/[Fe^{3+}]$ and $[H_2O_2]$/[substrate] on the photo-Fenton degradation of cationic azo dye Basic Blue 41. J Environ Sci Health A 45:622–629

Brillas E, Martínez-Huitle CA (2011) Synthetic diamond films: Preparation, electrochemistry, characterization and applications. Wiley, Hoboken

Brillas E, Bastida RM, Llosa E, Casado J (1995) Electrochemical destruction of aniline and 4–chloroaniline for wastewater treatment using a carbon–PTFE O_2–fed cathode. J Electrochem Soc 142: 1733–1741

Brillas E, Calpe JC, Casado J (2000) Mineralization of 2,4-D by advanced electrochemical oxidation processes. Water Res 34:2253–2262

Brillas E, Baños MA, Camps S, Arias C, Cabot P-L, Garrido JA, Rodríguez RM (2004) Catalytic effect of Fe^{2+}, Cu^{2+} and UVA light on the electrochemical degradation of nitrobenzene using an oxygen-diffusion cathode. New J Chem 28:314–322

Brillas E, Sirés I, Oturan MA (2009) Electro-Fenton process and related electrochemical technologies based on Fenton's reaction chemistry. Chem Rev 109:6570–6631

Bringas E, Saiz J, Ortiz I (2011) Kinetics of ultrasound-enhanced electrochemical oxidation of diuron on boron-doped diamond electrodes. Chem Eng J 172:1016–1022

Brown RF, Jamison SE, Pandit UK, Pinkus J, White GR, Braendlin HP (1964) The reaction of Fenton's reagent with phenoxyacetic acid and some halogen-substituted phenoxyacetic acids. J Org Chem 29: 146–153

Cañizares P, García-Gómez J, Sáez C, Rodrigo M (2003) Electrochemical oxidation of several chlorophenols on diamond electrodes: part I. Reaction mechanism. J Appl Electrochem 33:917–927

Cañizares P, García-Gómez J, Sáez C, Rodrigo M (2004) Electrochemical oxidation of several chlorophenols on diamond electrodes: part II. Influence of waste characteristics and operating conditions. J Appl Electrochem 34:87–94

Cañizares P, Díaz M, Domínguez JA, Lobato J, Rodrigo MA (2005a) Electrochemical treatment of diluted cyanide aqueous wastes. J Chem Technol Biotechnol 80:565–573

Cañizares P, Larrondo F, Lobato J, Rodrigo M, Sáez C (2005b) Electrochemical synthesis of peroxodiphosphate using boron-doped diamond anodes. J Electrochem Soc 152:D191–D196

Cañizares P, Lobato J, Paz R, Rodrigo M, Sáez C (2005c) Electrochemical oxidation of phenolic wastes with boron-doped diamond anodes. Water Res 39:2687–2703

Cañizares P, Paz R, Lobato J, Sáez C, Rodrigo MA (2006) Electrochemical treatment of the effluent of a fine chemical manufacturing plant. J Hazard Mater 138:173–181

Cañizares P, Lobato J, Paz R, Rodrigo MA, Sáez C (2007a) Advanced oxidation processes for the treatment of olive-oil mills wastewater. Chemosphere 67:832–838

Cañizares P, Larrondo F, Lobato J, Rodrigo MA, Saez C (2007 January 26) Síntesis electroquímica de sales de peroxodifosfato mediante electrodos de diamante conductor de la electricidad. Spanish Patent P200401820

Cañizares P, Sáez C, Sánchez-Carretero A, Rodrigo M (2009) Synthesis of novel oxidants by electrochemical technology. J Appl Electrochem 39:2143–2149

Chan PY, El-Din MG, Bolton JR (2012) A solar-driven UV/Chlorine advanced oxidation process. Water Res 46:5672–5682

Comninellis C, Nerini A (1995) Anodic oxidation of phenol in the presence of NaCl for wastewater treatment. J Appl Electrochem 25:23–28

Daghrir R, Drogui P, Robert D (2012a) Photoelectrocatalytic technologies for environmental applications. J Photochem Photobiol A 238: 41–52

Daghrir R, Drogui P, Khakani MAE (2012b) Photoelectrocatalytic oxidation of chlortetracycline using Ti/TiO_2 photo-anode with simultaneous H_2O_2 production. Electrochim Acta 87:18–31

Dai Q, Shen H, Xia Y, Chen F, Wang J, Chen J (2012) The application of a novel Ti/SnO_2-Sb_2O_3 PTFE-La-Ce-β-PbO_2 anode on the degradation of cationic gold yellow X-GL in sono-electrochemical oxidation system. Sep Purif Technol 104:9–16

Dhaouadi A, Adhoum N (2009) Degradation of paraquat herbicide by electrochemical advanced oxidation methods. J Electroanal Chem 637:33–42

Dirany A, Efremova Aaron S, Oturan N, Sirés I, Oturan MA, Aaron JJ (2011) Study of the toxicity of sulfamethoxazole and its degradation products in water by a bioluminescence method during application of the electro-Fenton treatment. Anal Bioanal Chem 400:353–360

Dirany A, Sirés I, Oturan N, Özcan A, Oturan MA (2012) Electrochemical treatment of the antibiotic sulfachloropyridazine: kinetics, reaction pathways, and toxicity evolution. Environ Sci Technol 46:4074–4082

Esclapez M, Sáez V, Milán-Yáñez D, Tudela I, Louisnard O, González-García J (2010) Sonoelectrochemical treatment of water polluted with trichloroacetic acid: from sonovoltammetry to pre-pilot plant scale. Ultrason Sonochem 17:1010–1020

Fang T, Liao L, Xu X, Peng J, Jing Y (2013) Removal of COD and colour in real pharmaceutical wastewater by photoelectrocatalytic oxidation method. Environ Technol 34(6):779–786

Fenton HJH (1894) Oxidation of tartaric acid in presence of iron. J Chem Soc Trans 65:899–910

Flannigan DJ, Suslick KS (2005) Plasma formation and temperature measurement during single-bubble cavitation. Nature 434:52–55

Flox C, Garrido JA, Rodríguez RM, Cabot P-L, Centellas F, Arias C, Brillas E (2007) Mineralization of herbicide mecoprop by photoelectro-Fenton with UVA and solar light. Catal Today 129: 29–36

Frontistis Z, Daskalaki VM, Katsaounis A, Poulios I, Mantzavinos D (2011) Electrochemical enhancement of solar photocatalysis: degradation of endocrine disruptor bisphenol-A on Ti/TiO_2 films. Water Res 45:2996–3004

Fryda M, Matthée T, Mulcahy S, Höfer M, Schäfer L, Tröster I (2003) Applications of DIACHEM electrodes in electrolytic water treatment. Electrochem Soc Interface 12:40–44

Gallard H, De Laat J, Legube B (1998) Effect of pH on the oxidation rate of organic compounds by Fe-II/H_2O_2. Mechanisms and simulation. New J Chem 22:263–268

Gandini D, Michaud PA, Duo I, Mahé E, Haenni W, Perret A, Comninellis C (1999) Electrochemical behavior of synthetic boron-doped diamond thin film anodes. New Diam Front C Tec 9: 303–316

Garbellini GS (2012) In: Kleperis J, Linkov V (eds) Electrolysis. InTech, Rijeka, pp 205–226

Garbellini GS, Salazar-Banda GR, Avaca LA (2008) Ultrasound applications in electrochemical systems: theoretical and experimental aspects. Quim Nova 31:123–133

Garbellini GS, Salazar-Banda GR, Avaca LA (2010) Effects of ultrasound on the degradation of pentachlorophenol by boron-doped diamond electrodes. Electrochim Acta 28:405–415

Garcia-Segura S, Garrido JA, Rodríguez RM, Cabot PL, Centellas F, Arias C, Brillas E (2012) Mineralization of flumequine in acidic medium by electro-Fenton and photoelectro-Fenton processes. Water Res 46:2067–2076

Garcia-Segura S, Dosta S, Guilemany JM, Brillas E (2013) Solar photoelectrocatalytic degradation of Acid Orange 7 azo dye using a highly stable TiO_2 photoanode synthesized by atmospheric plasma spray. Appl Catal B Environ 132-133:142–150

Georgieva J, Valova E, Armyanov S, Philippidis N, Poulios I, Sotiropoulos S (2012) Bi-component semiconductor oxide photoanodes for the photoelectrocatalytic oxidation of organic solutes and vapours: a short review with emphasis to TiO_2–WO_3 photoanodes. J Hazard Mater 211–212:30–46

Gogate PR, Pandit AB (2004) A review of imperative technologies for wastewater treatment I: oxidation technologies at ambient conditions. Adv Environ Res 8:501–551

González-García J, Banks CE, Šljukić B, Compton RG (2007) Electrosynthesis of hydrogen peroxide via the reduction of oxygen assisted by power ultrasound. Ultrason Sonochem 14:405–412

González-García J, Esclapez MD, Bonete P, Hernández YV, Garretón LG, Sáez V (2010) Current topics on sonoelectrochemistry. Ultrasonics 50:318–322

Guinea E, Garrido JA, Rodríguez RM, Cabot P-L, Arias C, Centellas F, Brillas E (2010) Degradation of the fluoroquinolone enrofloxacin by electrochemical advanced oxidation processes based on hydrogen peroxide electrogeneration. Electrochim Acta 55:2101–2115

Haber F, Weiss J (1934) The catalytic decomposition of hydrogen peroxide by iron salts. Proc R Soc Lond A Matter 147:332–351

Hiller R, Putterman SJ, Barber BP (1992) Spectrum of synchronous picosecond sonoluminescence. Phys Rev Lett 69:1182–1184

Irmak S, Yavuz HI, Erbatur O (2006) Degradation of 4-chloro-2-methylphenol in aqueous solution by electro-Fenton and photoelectro-Fenton processes. Appl Catal B Environ 63:243–248

Isarain-Chávez E, Arias C, Cabot PL, Centellas F, Rodríguez RM, Garrido JA, Brillas E (2010) Mineralization of the drug beta-blocker atenolol by electro-Fenton and photoelectro-Fenton using an air-diffusion cathode for H_2O_2 electrogeneration combined with a carbon-felt cathode for Fe^{2+} regeneration. Appl Catal B Environ 96:361–369

Isarain-Chávez E, Rodríguez RM, Cabot PL, Centellas F, Arias C, Garrido JA, Brillas E (2011) Degradation of pharmaceutical beta-blockers by electrochemical advanced oxidation processes using a flow plant with a solar compound parabolic collector. Water Res 45:4119–4130

Kapałka A, Fóti G, Comninellis C (2007) Investigations of electrochemical oxygen transfer reaction on boron-doped diamond electrodes. Electrochim Acta 53:1954–1961

Kapałka A, Lanova B, Baltruschat H, Fóti G, Comninellis C (2008) Electrochemically induced mineralization of organics by molecular oxygen on boron-doped diamond electrode. Electrochem Commun 10:1215–1218

Kaplan F, Hesenov A, Gözmen B, Erbatur O (2011) Degradations of model compounds representing some phenolics in olive mill wastewater via electro–Fenton and photoelectro–Fenton treatments. Environ Technol 32:685–692

Khataee AR, Vatanpour V, Amani Ghadim A (2009) Decolorization of CI Acid Blue 9 solution by UV/Nano-TiO_2, Fenton, Fenton-like, electro-Fenton and electrocoagulation processes: a comparative study. J Hazard Mater 161:1225–1233

Khataee AR, Zarei M, Asl SK (2010) Photocatalytic treatment of a dye solution using immobilized TiO_2 nanoparticles combined with photoelectro-Fenton process: optimization of operational parameters. J Electroanal Chem 648:143–150

Khataee AR, Zarei M, Khataee AR (2011) Electrochemical treatment of dye solution by oxalate catalyzed photoelectro-Fenton process using a carbon nanotube–PTFE cathode: optimization by central composite design. Clean Soil Air Water 39:482–490

Khataee AR, Safarpour M, Zarei M, Aber S (2012) Combined heterogeneous and homogeneous photodegradation of a dye using immobilized TiO_2 nanophotocatalyst and modified graphite electrode with carbon nanotubes. J Mol Catal A Chem 363:58–68

Lahkimi A, Oturan MA, Oturan N, Chaouch M (2007) Removal of textile dyes from water by the electro-Fenton process. Environ Chem Lett 5:35–39

Li H, Lei H, Yu Q, Li Z, Feng X, Yang B (2010) Effect of low frequency ultrasonic irradiation on the sonoelectro-Fenton degradation of cationic red X-GRL. Chem Eng J 160:417–422

Lin Y-T, Liang C, Chen J-H (2011) Feasibility study of ultraviolet activated persulfate oxidation of phenol. Chemosphere 82:1168–1172

Liu Y, Gan X, Zhou B, Xiong B, Li J, Dong C, Bai J, Cai W (2009) Photoelectrocatalytic degradation of tetracycline by highly effective TiO_2 nanopore arrays electrode. J Hazard Mater 171:678–683

Lorimer J, Mason T, Plattes M, Phull S, Walton D (2001) Degradation of dye effluent. Pure Appl Chem 73:1957–1968

Lucas MS, Dias AA, Sampaio A, Amaral C, Peres JA (2007) Degradation of a textile reactive azo dye by a combined chemical–biological process: Fenton's reagent-yeast. Water Res 41:1103–1109

Malpass GRP, Miwa DW, Machado SAS, Motheo AJ (2008) Decolourisation of real textile waste using electrochemical techniques: effect of electrode composition. J Hazard Mater 156:170–177

Marselli B, García-Gómez J, Michaud P-A, Rodrigo MA, Comninellis C (2003) Electrogeneration of hydroxyl radicals on boron-doped diamond electrodes. J Electrochem Soc 150:D79–D83

Martín de Vidales MJ, Sáez C, Cañizares P, Rodrigo MA (2012) Removal of triclosan by conductive–diamond electrolysis and sonoelectrolysis. J Chem Technol Biotechnol 88:823–828

Martínez SS, Uribe EV (2012) Enhanced sonochemical degradation of azure B dye by the electroFenton process. Ultrason Sonochem 19:174–178

Martínez-Huitle CA, Brillas E (2009) Decontamination of wastewaters containing synthetic organic dyes by electrochemical methods: a general review. Appl Catal B Environ 87:105–145

Martínez-Huitle CA, Ferro S (2006) Electrochemical oxidation of organic pollutants for the wastewater treatment: direct and indirect processes. Chem Soc Rev 12:1324–1340

Moreira FC, Garcia-Segura S, Vilar VJP, Boaventura RAR, Brillas E (2013) Decolorization and mineralization of sunset yellow FCF azo dye by anodic oxidation, electro-Fenton, UVA photoelectro-Fenton and solar photoelectro-Fenton processes. Appl Catal B Environ 142–143:877–890

Nissen S, Alexander BD, Dawood I, Tillotson M, Wells RP, Macphee DE, Killham K (2009) Remediation of a chlorinated aromatic hydrocarbon in water by photoelectrocatalysis. Environ Pollut 157:72–76

Oliver BG, Carey JH (1977) Photochemical production of chlorinated organics in aqueous solutions containing chlorine. Environ Sci Technol 11:893–895

Osugi ME, Zanoni MVB, Chenthamarakshan CR, de Tacconi NR, Woldemariam GA, Mandal SS, Rajeshwar K (2008) Toxicity assessment and degradation of disperse azo dyes by photoelectrocatalytic oxidation on Ti/TiO_2 nanotubular array electrodes. J Adv Oxid Technol 11:425–434

Oturan MA (1999) Hydroxylation of aromatic drugs by the electro-Fenton method. Formation and identification of the metabolites of Riluzole. New J Chem 23:793–794

Oturan MA (2000) An ecologically effective water treatment technique using electrochemically generated hydroxyl radicals for in situ destruction of organic pollutants: application to herbicide 2,4-D. J Appl Electrochem 30:475–482

Oturan MA, Pinson J, Deprez D, Terlain B (1992) Polyhydroxylation of salicylic acid by electrocheically generated OH radicals. New J Chem 16:705–710

Oturan MA, Sirés I, Oturan N, Pérocheau S, Laborde J-L, Trévin S (2008) Sonoelectro-Fenton process: a novel hybrid technique for the destruction of organic pollutants in water. J Electroanal Chem 624: 329–332

Oturan N, Panizza M, Oturan MA (2009) Cold incineration of chlorophenols in aqueous solution by advanced electrochemical process electro-Fenton. Effect of number and position of chlorine atoms on the degradation kinetics. J Phys Chem A 113:10988–10993

Oturan N, Zhou M, Oturan MA (2010) Metomyl degradation by electro-Fenton and electro-Fenton-like processes: a kinetics study of the effect of the nature and concentration of some transition metal ions as catalyst. J Phys Chem A 114:10605–10611

Oturan MA, Oturan N, Edelahi MC, Podvorica FI, Kacemi KE (2011) Oxidative degradation of herbicide diuron in aqueous medium by Fenton's reaction based advanced oxidation processes. Chem Eng J 171:127–135

Oturan N, Brillas E, Oturan MA (2012) Unprecedented total mineralization of atrazine and cyanuric acid by anodic oxidation and electro-Fenton with a boron-doped diamond anode. Environ Chem Lett 10: 165–170

Özcan A, Şahin Y, Koparal AS, Oturan MA (2008) Degradation of picloram by the electro-Fenton process. J Hazard Mater 153:718–727

Panizza M, Cerisola G (2001) Removal of organic pollutants from industrial wastewater by electrogenerated Fenton's reagent. Water Res 35:3987–3992

Panizza M, Cerisola G (2003) Electrochemical oxidation of 2-naphthol with in situ electrogenerated active chlorine. Electrochim Acta 48: 1515–1519

Panizza M, Cerisola G (2005) Application of diamond electrodes to electrochemical processes. Electrochim Acta 51:191–199

Panizza M, Cerisola G (2008) Electrochemical degradation of methyl red using BDD and PbO_2 anodes. Ind Eng Chem Res 47:6816–6820

Panizza M, Cerisola G (2009a) Direct and mediated anodic oxidation of organic pollutants. Chem Rev 109:6541–6569

Panizza M, Cerisola G (2009b) Electrochemical degradation of gallic acid on a BDD anode. Chemosphere 77:1060–1064

Panizza M, Cerisola G (2010) Applicability of electrochemical methods to carwash wastewaters for reuse. Part 1: anodic oxidation with diamond and lead dioxide anodes. J Electroanal Chem 638:28–32

Panizza M, Oturan MA (2011) Degradation of Alizarin Red by electro-Fenton process using a graphite-felt cathode. Electrochim Acta 56: 7084–7087

Panizza M, Duo I, Michaud P, Cerisola G, Comnellis C (2000) Electrochemical generation of silver (II) at boron–doped diamond electrodes. Electrochem Solid-State 3:550–551

Panizza M, Michaud P, Cerisola G, Comninellis C (2001) Electrochemical treatment of wastewaters containing organic pollutants on boron-doped diamond electrodes: prediction of specific energy consumption and required electrode area. Electrochem Commun 3:336–339

Panizza M, Zolezzi M, Nicolella C (2006) Biological and electrochemical oxidation of naphthalene sulfonates in a contaminated site leachate. J Chem Technol Biotechnol 81:225–232

Panizza M, Sirés I, Cerisola G (2008) Anodic oxidation of mecoprop herbicide at lead dioxide. J Appl Electrochem 38:923–929

Park H, Bak A, Ahn YY, Choi J, Hoffmannn MR (2012) Photoelectrochemical performance of multi-layered BiO_x–TiO_2/Ti electrodes for degradation of phenol and production of molecular hydrogen in water. J Hazard Mater 211:47–54

Pelegrini R, Reyes J, Durán N, Zamora PP, De Andrade AR (2000) Photoelectrochemical degradation of lignin. J Appl Electrochem 30:953–958

Peralta-Hernández J, Meas-Vong Y, Rodríguez FJ, Chapman TW, Maldonado MI, Godínez LA (2006) In situ electrochemical and photo-electrochemical generation of the fenton reagent: a potentially important new water treatment technology. Water Res 40:1754–1762

Peralta-Hernández JM, Meas-Vong Y, Rodríguez FJ, Chapman TW, Maldonado MI, Godínez LA (2008) Comparison of hydrogen peroxide-based processes for treating dye-containing wastewater: decolorization and destruction of Orange II azo dye in dilute solution. Dyes Pigments 76:656–662

Phutdhawong W, Chowwanapoonpohn S, Buddhasukh D (2000) Electrocoagulation and subsequent recovery of phenolic compounds. Anal Sci 16:1083–1084

Pignatello JJ, Oliveros E, MacKay A (2006) Advanced oxidation processes for organic contaminant destruction based on the Fenton reaction and related chemistry. Crit Rev Environ Sci Technol 36: 1–84

Pimentel M, Oturan N, Dezotti M, Oturan MA (2008) Phenol degradation by advanced electrochemical oxidation process electro-Fenton using a carbon felt cathode. Appl Catal B Environ 83:140–149

Polcaro AM, Mascia M, Palmas S, Vacca A (2002) Kinetic study on the removal of organic pollutants by an electrochemical oxidation process. Ind Eng Chem Res 41:2874–2881

Polcaro AM, Vacca A, Palmas S, Mascia M (2003) Electrochemical treatment of wastewater containing phenolic compounds: oxidation at boron-doped diamond electrodes. J Appl Electrochem 33:885–892

Polcaro AM, Vacca A, Mascia M, Palmas S (2005) Oxidation at boron doped diamond electrodes: an effective method to mineralise triazines. Electrochim Acta 50:1841–1847

Polcaro AM, Vacca A, Mascia M, Palmas S, Ruiz JR (2009) Electrochemical treatment of waters with BDD anodes: kinetics of the reactions involving chlorides. J Appl Electrochem 39:2083–2092

Rodriguez J, Rodrigo MA, Panizza M, Cerisola G (2009) Electrochemical oxidation of acid yellow 1 using diamond anode. J Appl Electrochem 39:2285–2289

Rooze J, Rebrov EV, Schouten JC, Keurentjes JT (2013) Dissolved gas and ultrasonic cavitation—a review. Ultrason Sonochem 20(1):1–11

Ruiz EJ, Ortega-Borges R, Jurado JL, Chapman T, Meas Y (2009) Simultaneous anodic and cathodic production of sodium percarbonate in aqueous solution. Electrochem Solid-State 12:E1–E4

Ruiz EJ, Arias C, Brillas E, Hernández-Ramírez A, Peralta-Hernández JM (2011a) Mineralization of Acid Yellow 36 azo dye by electro-Fenton and solar photoelectro-Fenton processes with a boron-doped diamond anode. Chemosphere 82:495–501

Ruiz EJ, Hernández-Ramírez A, Peralta-Hernández JM, Arias C, Brillas E (2011b) Application of solar photoelectro-Fenton technology to azo dyes mineralization: effect of current density, Fe^{2+} and dye concentrations. Chem Eng J 171:385–392

Sáez C, Rodrigo MA, Cañizares P (2008) Electrosynthesis of ferrates with diamond anodes. AIChE J 54:1600–1607

Sáez C, Cañizares P, Sánchez-Carretero A, Rodrigo M (2010a) Electrochemical synthesis of perbromate using conductive-diamond anodes. J Appl Electrochem 40:1715–1719

Sáez V, Esclapez MD, Tudela I, Bonete P, Louisnard O, González-García J (2010b) 20 kHz sonoelectrochemical degradation of perchloroethylene in sodium sulfate aqueous media: Influence of the operational variables in batch mode. J Hazard Mater 183:648–654

Sáez V, Tudela I, Esclapez MD, Bonete P, Louisnard O, González-García J (2011) Sonoelectrochemical degradation of perchloroethylene in water: enhancement of the process by the absence of background electrolyte. Chem Eng J 168:649–655

Salazar R, Garcia-Segura S, Ureta-Zañartu MS, Brillas E (2011) Degradation of disperse azo dyes from waters by solar photoelectro-Fenton. Electrochim Acta 56:6371–6379

Salazar R, Brillas E, Sirés I (2012) Finding the best Fe^{2+}/Cu^{2+} combination for the solar photoelectro-Fenton treatment of simulated wastewater containing the industrial textile dye Disperse Blue 3. Appl Catal B Environ 115-116:107–116

Sánchez-Carretero A, Sáez C, Cañizares P, Rodrigo M (2011) Electrochemical production of perchlorates using conductive diamond electrolyses. Chem Eng J 166:710–714

Sapkal RT, Shinde SS, Mahadik MA, Mohite VS, Waghmode TR, Govindwar SP, Rajpure KY, Bhosale CH (2012) Photoelectrocatalytic decolorization and degradation of textile effluent using ZnO thin films. J Photochem Photobiol B 114:102–107

Scott-Emuakpor E, Kruth A, Todd M, Raab A, Paton G, Macphee D (2012) Remediation of 2,4-dichlorophenol contaminated water by visible light-enhanced WO_3 photoelectrocatalysis. Appl Catal B Environ 123–124:433–439

Serrano K, Michaud P, Comninellis C, Savall A (2002) Electrochemical preparation of peroxodisulfuric acid using boron doped diamond thin film electrodes. Electrochim Acta 48:431–436

Shih Y-J, Putra WN, Huang Y–H, Tsai J–C (2012) Mineralization and deflourization of 2,2,3,3-tetrafluoro-1-propanol (TFP) by UV/persulfate oxidation and sequential adsorption. Chemosphere 89: 1262–1266

Siddique M, Farooq R, Khan ZM, Khan Z, Shaukat S (2011) Enhanced decomposition of reactive blue 19 dye in ultrasound assisted electrochemical reactor. Ultrason Sonochem 18:190–196

Sirés I, Brillas E (2012) Remediation of water pollution caused by pharmaceutical residues based on electrochemical separation and degradation technologies: a review. Environ Int 40:212–229

Sirés I, Garrido JA, Rodríguez RM, Cabot PL, Centellas F, Arias C, Brillas E (2006a) Electrochemical degradation of paracetamol from water by catalytic action of Fe^{2+}, Cu^{2+}, and UVA light on electrogenerated hydrogen peroxide. J Electrochem Soc 153:D1–D9

Sirés I, Cabot PL, Centellas F, Garrido JA, Rodríguez RM, Arias C, Brillas E (2006b) Electrochemical degradation of clofibric acid in water by anodic oxidation: comparative study with platinum and boron-doped diamond electrodes. Electrochim Acta 52:75–85

Sirés I, Garrido JA, Rodríguez RM, Brillas E, Oturan N, Oturan MA (2007a) Catalytic behavior of the Fe^{3+}/Fe^{2+} system in the electro-Fenton degradation of the antimicrobial chlorophene. Appl Catal B Environ 72:382–394

Sirés I, Oturan N, Oturan MA, Rodríguez RM, Garrido JA, Brillas E (2007b) Electro-Fenton degradation of antimicrobials triclosan and triclocarban. Electrochim Acta 52:5493–5503

Sirés I, Centellas F, Garrido JA, Rodríguez RM, Arias C, Cabot P-L, Brillas E (2007c) Mineralization of clofibric acid by electrochemical advanced oxidation processes using a boron-doped diamond anode and Fe^{2+} and UVA light as catalysts. Appl Catal B Environ 72:373–381

Sirés I, Oturan N, Oturan MA (2010) Electrochemical degradation of β-blockers. Studies on single and multicomponent synthetic aqueous solutions. Water Res 44:3109–3120

Skoumal M, Rodriguez RM, Cabot PL, Centellas F, Garrido JA, Arias C, Brillas E (2009) Electro-Fenton, UVA photoelectro-Fenton and solar photoelectro-Fenton degradation of the drug ibuprofen in acid aqueous medium using platinum and boron-doped diamond anodes. Electrochim Acta 54:2077–2085

Sun Y, Pignatello JJ (1993a) Activation of hydrogen peroxide by iron (III) chelates for abiotic degradation of herbicides and insecticides in water. J Agric Food Chem 41:308–312

Sun Y, Pignatello JJ (1993b) Photochemical reactions involved in the total mineralization of 2,4-D by iron (3+)/hydrogen peroxide/UV. Environ Sci Technol 27:304–310

Tsitonaki A, Petri B, Crimi M, Mosbæk H, Siegrist RL, Bjerg PL (2010) In situ chemical oxidation of contaminated soil and groundwater using persulfate: a review. Crit Rev Environ Sci Technol 40:55–91

Urtiaga A, Rueda A, Anglada Á, Ortiz I (2009) Integrated treatment of landfill leachates including electrooxidation at pilot plant scale. J Hazard Mater 166:1530–1534

Walling C (1998) Intermediates in the reactions of Fenton type reagents. Acc Chem Res 31:155–157

Wang A, Qu J, Liu H, Ru J (2008) Mineralization of an azo dye Acid Red 14 by photoelectro-Fenton process using an activated carbon fiber cathode. Appl Catal B Environ 84:393–399

Wang A, Li Y-Y, Estrada AL (2011) Mineralization of antibiotic sulfamethoxazole by photoelectro-Fenton treatment using activated carbon fiber cathode and under UVA irradiation. Appl Catal B Environ 102:378–386

Weiss E, Groenen-Serrano K, Savall A (2008a) A comparison of electrochemical degradation of phenol on boron doped diamond and lead dioxide anodes. J Appl Electrochem 38:329–337

Weiss E, Sáez C, Groenen-Serrano K, Cañizares P, Savall A, Rodrigo M (2008b) Electrochemical synthesis of peroxomonophosphate using boron-doped diamond anodes. J Appl Electrochem 38:93–100

Xie Y-B, Li X (2006) Interactive oxidation of photoelectrocatalysis and electro-Fenton for azo dye degradation using TiO_2–Ti mesh and reticulated vitreous carbon electrodes. Mater Chem Phys 95:39–50

Xin Y, Liu H, Han L, Zhou Y (2011) Comparative study of photocatalytic and photoelectrocatalytic properties of alachlor using different morphology TiO_2/Ti photoelectrodes. J Hazard Mater 192:1812–1818

Zhang H, Zhang D, Zhou J (2006) Removal of COD from landfill leachate by electro-Fenton method. J Hazard Mater 135:106–111

Zhang Z, Yuan Y, Liang L, Cheng Y, Shi G, Jin L (2008) Preparation and photoelectrocatalytic activity of ZnO nanorods embedded in highly ordered TiO_2 nanotube arrays electrode for azo dye degradation. J Hazard Mater 158:517–522

Zhang A, Zhou M, Liu L, Wang W, Jiao Y, Zhou Q (2010) A novel photoelectrocatalytic system for organic contaminant degradation on a TiO_2 nanotube (TNT)/Ti electrode. Electrochim Acta 55:5091–5099

Zhao X, Qu J, Liu H, Qiang Z, Liu R, Hu C (2009) Photoelectrochemical degradation of anti-inflammatory pharmaceuticals at Bi_2MoO_6–boron-doped diamond hybrid electrode under visible light irradiation. Appl Catal B Environ 91:539–545

Zhao H, Wang Y, Wang Y, Cao T, Zhao G (2012) Electro-fenton oxidation of pesticides with a novel Fe_3O_4@Fe_2O_3/activated carbon aerogel cathode: high activity, wide pH range and catalytic mechanism. Appl Catal B-Environ 125:120–127

Zhou M, Tan Q, Wang Q, Jiao Y, Oturan N, Oturan MA (2012) Degradation of organics in reverse osmosis concentrate by electro-Fenton process. J Hazard Mater 215–216:287–293